



HUYGENS

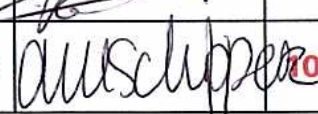
**TITLE: HUYGENS PRE-SEPARATION HEALTH ASSESSMENT
AND OPERATIONS SYNTHESIS REPORT**

Doc n° HUY.ASPI.MIS.RE.0002

Ed. : n° 02

Date: 10/05/05

Rev. : n° 01

	FUNCTION	NAME	SIGNATURE	DATE
WRITTEN BY	TECHNICAL TEAM	R.DUPRE / P.COUZIN		10/05/05
APPROVED BY	PROGRAM MANAGER	AM SCHIPPER		10/05/05

CLASSES DE CONFIDENTIALITE	SOCIETE	MILITAIRE	PROGRAMME		
	Non Protégé : <input type="checkbox"/> Réservé Alcatel : <input type="checkbox"/> Confid. Alcatel : <input type="checkbox"/> Secret AS : <input type="checkbox"/>	Non Protégé : <input type="checkbox"/> Diff. Restreinte : <input type="checkbox"/> Confid. Défense : <input type="checkbox"/> Secret Défense : <input type="checkbox"/>	Classe 1/Grand Public : <input type="checkbox"/> Classe 2/Industrie : <input type="checkbox"/> Classe 3/Diff. Restr. : <input type="checkbox"/> Classe 4/Confidentiel : <input type="checkbox"/>		
CONTRAT ou MARCHÉ (Note Externe)	Client ESA	n° contrat ou marché 12 150/96/NL/RE	Programme HUYGENS		
	Document Contractuel -	Lot -	Poste -		
TITRE	HUYGENS PRE-SEPARATION HEALTH ASSESSMENT AND OPERATIONS SYNTHESIS REPORT		Catégorie de configuration Configuré : <input type="checkbox"/> Non configuré : <input type="checkbox"/>		
AUTEUR Sigle : Nom : P. Couzin / R. Dupré Signature					
Date 10/05/05	Réf. interne/Ed. 1	Réf. Programme/Ed. HUYGENS	Nb pages 54	Nb d'annexes 0	
RESUME D'AUTEUR Ce document présente l'évaluation technique de la sonde Huygens résultant des opérations qui ont précédé sa séparation de Cassini. .					
Références Informatiques	Réf. du fichier : Nom du logiciel : WORD 97	Langue du document : Ang Langue faisant foi : Ang			
ETAT DES EDITIONS					
N°	DATE	RAISON DE L'EVOLUTION			
1		Création -			
MOTS CLES HUYGENS CRUISE CHECK OUT					
		Catégorie de diffusion			
		INTERET		Sigle : Nom : Signature	
		Court terme : <input type="checkbox"/> Moyen et long termes : <input type="checkbox"/>			
		DIFFUSION SUPPLEMENTAIRE		Sigle : Nom : Signature	
		Autorisée : <input type="checkbox"/> Contrôlée : <input type="checkbox"/>			

Internal Diffusion Sheet

P. MAUTE	X
A.-M. SCHIPPER	X
P. COUZIN	X
G. ROUYER	X
R. DUPRE	X
G. CLUZET	X

Change Notice

ED.	REV.	DATES	MODIFIED PAGES	CHANGES	APPROVAL
01	00	24/11/04		1 st issue	
02	00	07/12/04		This issue includes the analysis of the 2 nd batteries depassivation phase.	
02	01	10/05/05		Includes ESA comments made on 13/12/04	

TABLE OF CONTENTS

1. SCOPE	1
2. APPLICABLE DOCUMENTS.....	2
3. LIST OF ABBREVIATIONS	4
4 CONFIGURATION	7
4.1 CHECKOUT CHARACTERISTICS	7
4.2 PROBE CHECKOUT SCENARIO'S	10
4.2.1 CO1 checkouts	10
4.2.2 CO2 checkouts	12
5. FLIGHT CHECKOUTS.....	13
5.1 TELECOMMANDING.....	13
5.2 TELEMETRY FRAMES AND PACKETS STRUCTURE	16
5.3 TELECOMMUNICATION	16
185.4 POWER	19
5.4.1 Checkouts	19
5.4.2 Depassivation	24
245.5 DATA HANDLING.....	30
5.6 ON BOARD SOFTWARE	36
5.6.1.SASW	36
5.6.2 POSW	38

5.7 TEMPERATURE EVOLUTION	39
5.7.1 Cassini temperature sensors	39
5.7.2 Probe temperatures	40
5.8 EXPERIMENTS STATUS WORD	45
6. CASSINI CHECKOUTS.....	46
7. CONCLUSION	47

1. SCOPE

The present report covers the flight cruise checkouts performed in the frame of the phase F of the Huygens probe, including the last F16 checkout as well as the first and second battery depassivations.

This document aims at giving a technical overview of the behavior of the Huygens Probe System and subsystems during the flight checkouts in order to support the mission go/nogo decision process.

Note that experiments behavior analysis is not part of this report.

2. APPLICABLE DOCUMENTS

The tests have been performed according to the following documents:

- AD01: ESOC checkout sequences
- AD02: Spacecraft Data Operations Handbook (SDOH) DOPS-SMD-HUY-DB-004, Issue 1.0, June 1996

Reference documents for the present report are:

- RD01: T° Flight Prediction Report
Doc. n° HUY.MBB.340.AN.0045, Issue 03
- RD02: Thermal model adjustment and recalculation of temperatures
Doc. n° TN-RIA54-98-0018-A, 07/07/98
- RD03: Huygens Flight checkout F1 & F2 test report
Doc. n° HUY.AS/c.100 .TR .600
- RD04: Huygens Flight checkout F3 test report
Doc. n° HUY.AS/c.100 .TR .601
- RD05: Huygens Flight checkout F4 test report
Doc. n° HUY.AS/c.100 .TR .602
- RD06: Huygens Flight checkout F5 test report
Doc. n° HUY.AS/c.100 .TR .603
- RD07: Huygens Flight checkout F6 test report
Doc. n° HUY.AS/c.100 .TR .604
- RD08: Huygens Flight checkout F7 test report
Doc. n° HUY.AS/c.100 .TR .605
- RD09: Huygens Flight checkout F8 test report
Doc. n° HUY.ASPI.HIT.RE.0001
- RD10: Huygens Flight checkout F9 test report
Doc. n° HUY.ASPI.HIT.RE.0002
- RD11: Huygens F10 Checkout Operational Report
Doc. n° TOS-OF-HFR-010

- RD12: Huygens F11 Checkout Operational Report
Doc. n° TOS-OF-HFR-011
- RD13: Huygens Recovery Task Force (HRTF) Final Report
Doc. n° HUY-RP-12241
- RD14: Huygens Entry – Impact of Stiction on Accelerometer Unit
Doc. n° HUY-ASP-MIS-TN-0004
- RD15 : Probe Flight temperatures prediction for the pre heating scenario
Doc. ESA n° HUY-TN-199 Rev.1.2

3. LIST OF ABBREVIATIONS

ACP	Aerosol Collector and Pyrolyzer
AGC	Automatic Gain Control
APIS	Acoustic Sounder (SSP experiment)
BC	Back Cover
BDR	Battery Discharge Regulator
CASU	Central Acceleration Sensor Unit
CCD	Charge Coupled Device
CDMS	Command and Data Management Subsystem
CDMU	Command and Data Management Unit
CDS	Command and Data Subsystem (of the orbiter)
CO	Check Out
CRID	
CUT	Computed Unit of Time
DC	Down Converter
DDB	Descent Data Broadcast
DISR	Descent Imager and Spectral Radiometer
DMA	Direct Memory Access
DSN	Deep Space Network
DT	Dead Time
DWE	Doppler Wind Experiment
EDAC	Error Detection And Correction
EEPROM	Electrically Erasable Programmed Read Only Memory
EMC	Electro-Magnetic Compatibility
ESOC	European Space Operations Center
ESTEC	European Space Research and Technology Center
FDI	Frame Data Interface
FS	Front Shield
GCMS	Gas Chromatograph and Mass Spectrometer
HASI	Huygens Atmosphere Structure Instrument
HGA	High Gain Antenna

HK	House Keeping
IR	Infra-Red
JPL	Jet Propulsion Laboratory
LGA	Low Gain Antenna
LNA	Low Noise Amplifier
LSB	Least Significant Bit
MTT	Mission Timeline Table
MTU	Mission Timer Unit
MVDA	
NCO	Numerically Controlled Oscillator
PCDU	Power Conditioning and Distribution Unit
PDD	Parachute Deployment Device
PI	Principal Investigator
PJM	Parachute Jettison Mechanism
POSW	Probe On-board SoftWare
PRT	Probe Relay Test
PSA	Probe Support Avionics
PSE	Probe Support Equipment
RAM	Random Access Memory
RF	Radio Frequency
RFE	Radio Front End
RSS	Radio Science experiment
RSW	Receiver Software
RT	Real Time
RTI	Real Time Interrupt
RUSO	Receiver Ultra Stable Oscillator
SASW	Support Avionics SoftWare
SEPS	SEParations Subsystem
SSP	Surface Science Package
TAT	Time Altitude Table
TC	TeleCommand
TCXO	Transmitter Compensated Crystal Oscillator
TM	TeleMetry
TUSO	Transmitter Ultra Stable Oscillator

TX Transmitter
USO Ultra Stable Oscillator

4 CONFIGURATION

4.1 CHECKOUT CHARACTERISTICS

The Table 4.1-1 below indicates for each checkout the date, the delay from launch, the type, the next event and the delay before this event, the duration, the relative distances to Sun and Earth, and the Sun-Spacecraft-Earth angle.

Number	Date	Month # after launch	Type	Next event	Delay before next event	duration	Distance to Sun (AU)	Distance to Earth (AU)	Sun-S/C-Earth angle (°)
1	23/10/1997	0	CO2				1	0	
2	27/03/1998	6	CO1			3h04	0.6		
3	22/12/1998	14	CO2			3h37	1.6		
4	14/09/1999	23	CO1 b			3h47	1.3	0.3	0
5	2/2/2000	28	CO2	PRT1	1 day	3h39	2.7	2.9	19.5
6	28/7/2000	34	CO1 a	PRT2	6 months	3h28	4.1	4.6	10
7	22/03/2001	41	CO2	PRT3	3 months	3h49	5.5	5.8	10
8	20/09/2001	47	CO1 b	PRT4	2 months	4h19	6.4	6	10
9	15/04/2002	53	CO2			5h02	7.2	7.7	7
10	16/09/2002	58	CO1 a	PRT5		5h44	7.7	7.7	7
11	03/05/2003	66	CO2			5h35	8.2	8.9	5.3
12	18/09/2003	70	CO1 b			5h35	8.5	8.9	5.5
Pre-Heating	04/12/2003	73	CO1 a			7h02	8.7	7.8	6
13	20/03/2003	77	CO1 b			3h03 MTU drift + 5h11	8.9	8.7	6.4
14	14/07/2004	81	CO2			2h MTU drift + 5h10	9	10	3.54
15	14/09/2004	83	CO1 b			5h10 + MTU red loading	9	9.5	6

1 st depassiva tion	19/9/2004	88				35mn	9	9.5	6
F16	23/11/04	90	CO1 b			5h10 + MTU red loading	9	8.46	6
2 nd depassiva tion	5/12/04	90				35mn	9	8,4	6

Table 4.1-1: Checkout summary

The “regular” checkouts, i.e. the checkouts that were part of the original Huygens phase F definition, are numbered from 1 to 15. The last of these checkouts, #16, was run on the 23rd of November 2004. Several checkout types are identified; they are addressed in the next chapter.

F3 occurred after the first Venus flyby, F4 after Earth flyby, F5 after crossing of the asteroid belt between Mars and Jupiter orbits, F7 after Jupiter flyby, F8 after Orbiter mute test, F14 after Saturn Orbit Insertion.

The orientation during checkout of the Orbiter-Z axis, which is the High Gain Antenna axis, was:

- towards the Sun up to F4 in order to have the High Gain Antenna shadowing the rest of the spacecraft
- then towards the Earth.

The probe was partially Sun illuminated during F6 and F7.

The distance of the Cassini spacecraft to the Sun is illustrated on Figure 4.1-1 for all checkouts.

The Cassini LGA-1 was the prime telecommunication antenna for F1 to F4 then HGA was the prime antenna for all remaining checkouts.

The data was down linked in near real time via JPL and DSN station for most checkouts. Only F9 and F10 data was down linked 2 days after the checkout sequence due to bad real time downlink conditions. Goldstone DSN station was used for all checkouts except F4 and F9 for which Madrid and Camberra stations were respectively used.

F15 was run just before the first battery depassivation sequence, which occurred on the 19/09/2004. The battery depassivation consisted in a power load application to each of the five batteries for a few minutes by switching on the probe instruments. The aim of this sequence is to break the passivation layer of the battery electrodes.

The Cassini instruments were switched off up to F7 then in sleep mode and muted from F8 to F16.

In addition to the regular checkouts, a number of flight tests have been carried out:

- the Probe Relay Tests (PRT) have been performed first to validate the Probe Support Avionics behavior in realistic RF link conditions. PRT 1 is the test which has allowed to discover the relay link design anomaly documented in RD13 (HRTF report). The subsequent PRT's have been run first to fully characterise the anomaly, then to quantify the benefit of the various candidate solutions. It shall be pointed out that the PRT's have only involved the Probe Support Avionics; the probe was off during those tests.

- The pre-heating test has been performed to validate in flight (i.e. on the FM probe system) the implementation of one of the two solutions selected to resolve the link anomaly problem, the so called "pre-heating".

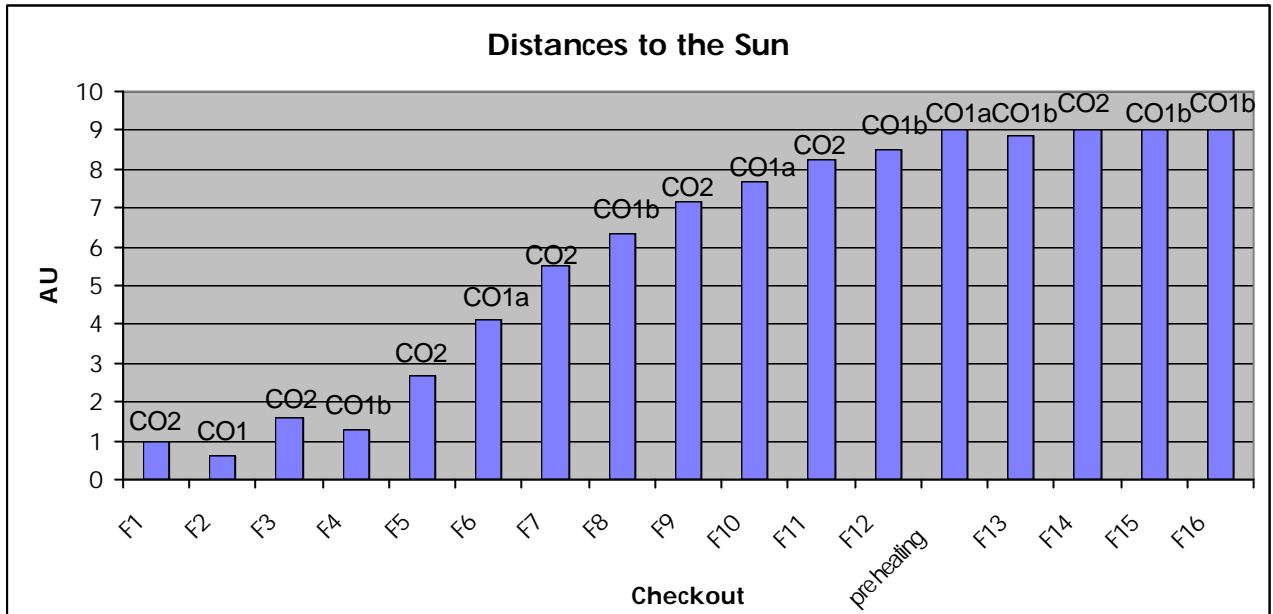


Figure 4.1-1: Cassini - Sun distance

The total duration of checkouts is represented on Figure 4.1-2, showing the progressive increase of this duration.

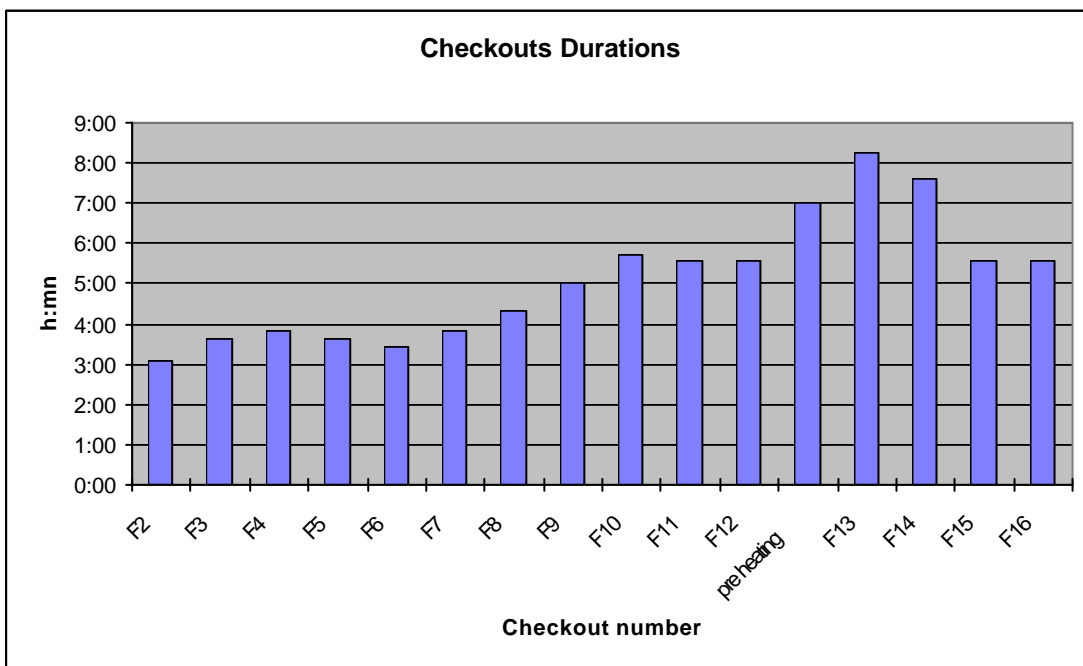


Figure 4.1-2: Checkouts duration

4.2 PROBE CHECKOUT SCENARIO'S

Two sequences were initially foreseen:

- The CO1 sequence, which consists in a Descent Simulation scenario (especially with DISR in "descent simulation mode") with spin profile simulated by telecommands. CO1 is run with chain A "valid" (see § 4.2.1)
- The CO2 sequence consisting in a Checkout scenario. CO2 is run with chain A "invalid" (see § 4.2.1).

F2, F4, F6, F8, F10, F12, F13, F15 and F16 are CO1 checkouts.

F1, F3, F5, F7, F9, F11 and F14 are CO2 checkouts.

The following operations were added to the original scenario for both CO1 and CO2 sequences:

- The repetition of the "flight check out alteration TC", mainly to avoid failures leading to have GCMS operating its valves during checkout
- POSW and SASW EPROM's dumps, to assess the EEPROM susceptibility to single particles
- Some modifications, on a case by case basis, requested by the Primary Investigators.

4.2.1 CO1 checkouts

Two other scenario's have been distinguished within the probe CO1 checkouts:

- The CO1a sequence, where the "a" indicates that the link on the chain A does not use TUSO and RUSO, as in the original CO1 sequence, but instead TCXO's. F6 and F10 are CO1a checkouts
- The CO1b sequence, where the "b" indicates that the link on the chain A uses TUSO and RUSO. F4, F8, F12, F13, F15 and F16 are CO1b checkouts (note that F2 was an original CO1 sequence).

In the following, chain A indicated "valid" means experiments are proposed to use the broadcast data from chain A (default configuration for CO1 type), chain A indicated "invalid" means experiments are proposed to use the broadcast data from chain B (default configuration for CO2 type).

For both F6 and F10 CO1a checkouts, the chain A was indicated as "valid" and the experiment operations were:

- HASI and SSP simulated descent then SSP specific investigation on APIS
- ACP in dormant mode then in "mechanisms check mode" in the second part of the simulated descent
- GCMS simulated descent with valves disabled by TCs

- DISR descent with spin simulation by TCs and EEPROM dump.

During F10, DISR performed in addition a specific sequence at the end of descent.

For both F4 and F8 CO1b checkouts, the chain A was indicated as "valid" and the experiment operations were identical to CO1a ones at the exception of the DISR EEPROM dump, which was not done.

In addition, F4 included special commands to open the ACP P2 valve and F8 DISR specific investigation at the end of the sequence.

F12 was based on F8, with

- CCD measurements and new EEPROM patches/dumps for DISR
- EEPROM patch/dump in pre-T₀ for GCMS.

After the implementation of the pre-heating patch in December 2003 (see "pre-heating" in Table 4.1-1), the method used to force the μ processor flag to invalid for the simulated descent phase could not be used anymore except by running a checkout including a full pre-heating duration (4h00). After the validation of the correct pre heating implementation, it was decided not to extend the "pre-T₀" duration for the subsequent checkouts (F13 to F16) because:

- it was not bringing any value to the validation already performed
- it was leading to high unit's temperature at the end of the checkout.

As a consequence, F13, F15 and F16 checkouts have been run with both chains declared "valid".

F13 was based on F8 and F12, with

- CCD and IR measurements and new EEPROM patches/dumps for DISR
- HASI added a new CRID file.

A specific MTU drift test was run just before F13 in a separate power cycle, the MTU timers were then activated for the first time from September 1997.

F15 sequence was based on F13 with three instrument related changes: DISR CCD and IR measurements and new EEPROM patches/dumps using new CRID, ACP added out-gassing commands, SSP added new CRID with an extra power cycle. Within the same power cycle, the MTU redundant loading sequence was run at the end of checkout, enabling in the same time the extended observation of chain A carrier frequency modulation with TUSO.

F16 sequence was essentially identical to F15 with the noticeable exception of the ACP Gate Valve Lock command added to the sequence.

4.2.2 CO2 checkouts

For F1, F3, F5, F7, F9 and F11 CO2 checkouts, the chain A was indicated as "invalid" during the simulated descent phase. F14 checkout, which occurred after the pre-heating patch, has been run with both chains declared "valid".

The link on the chain A has used the TUSO and RUSO.

A specific MTU drift test has been run just before F14.

The experiment specific operations were:

- HASI and SSP simulated descent. SSP performed specific investigation on APIS from F3 to characterize an anomaly noticed of the acoustic sounder (ringing effect – see SSP dedicated reports)
- ACP in dormant mode (F7, F9) or engineering mode (F11) then in "mechanisms check mode" in the second part of the simulated descent
- GCMS calibration sequence
- DISR calibration sequences 1 and 2 then in F7, EEPROM upload; 4 IR spectrometers exposures inserted in F9
- DISR and HASI patch related to pre-heating applied in F11 (full validation was performed within the dedicated pre-heating test in December 2003)
- F9, F11 increased by one hour to better characterize the USO's low frequency oscillations with TUSO remaining on during this extra hour.

5. FLIGHT CHECKOUTS

The analyses of the flight checkouts have been based both on engineering data plots, and on dedicated telemetry stream extracts ("MVDA files") produced by ESOC after each checkout.

The main outcomes of the as-run sequence evaluation are, for all checkouts:

- The timing requested by the scenario was correctly followed by the Cassini CDS and all TC's sent by ground via the test sequence were correctly executed for both chains
- The mission timeline run autonomously on board Huygens was correctly executed.

The following paragraphs present the analysis of checkouts, per function.

5.1 TELECOMMANDING

The analysis of the reported PSA, CDMU A and B telecommand counters, and of the reported CDMU's Mission timeline commands counts provides a good overview of the execution of the checkout sequences, and of the mission timeline.

Note that, nominally, typical CO2 sequences stored in Cassini for execution contain some 1690 TC's while typical CO1 sequences contain some 410 TC's. These include TC's for the PSA A and B and TC's for the CDMU A and B.

The Figures 5.1-1 and 5.1-2 hereafter show, as examples, the evolution of the different counters along the two last F14 (CO2) and F15 (CO1) checkouts, where the time "0" corresponds to the start of sequence, i.e. the turn on of the PSA A and B. In this time scale, So event (the software entry event) is declared at t=**3600s**.

For all checkouts:

- All ground telecommands have been accepted as valid, both on PSA's and CDMU's side
- More telecommands have been sent to PSA A. This is nominal and due to the numerous commands for switching to basic frequency on chain A
- Exactly the same number of valid TC's have been forwarded to CDMU A and B
- The evolution of the automatic command counts, identical for channels A and B is in line with the stored Mission Timeline Table (MTT).

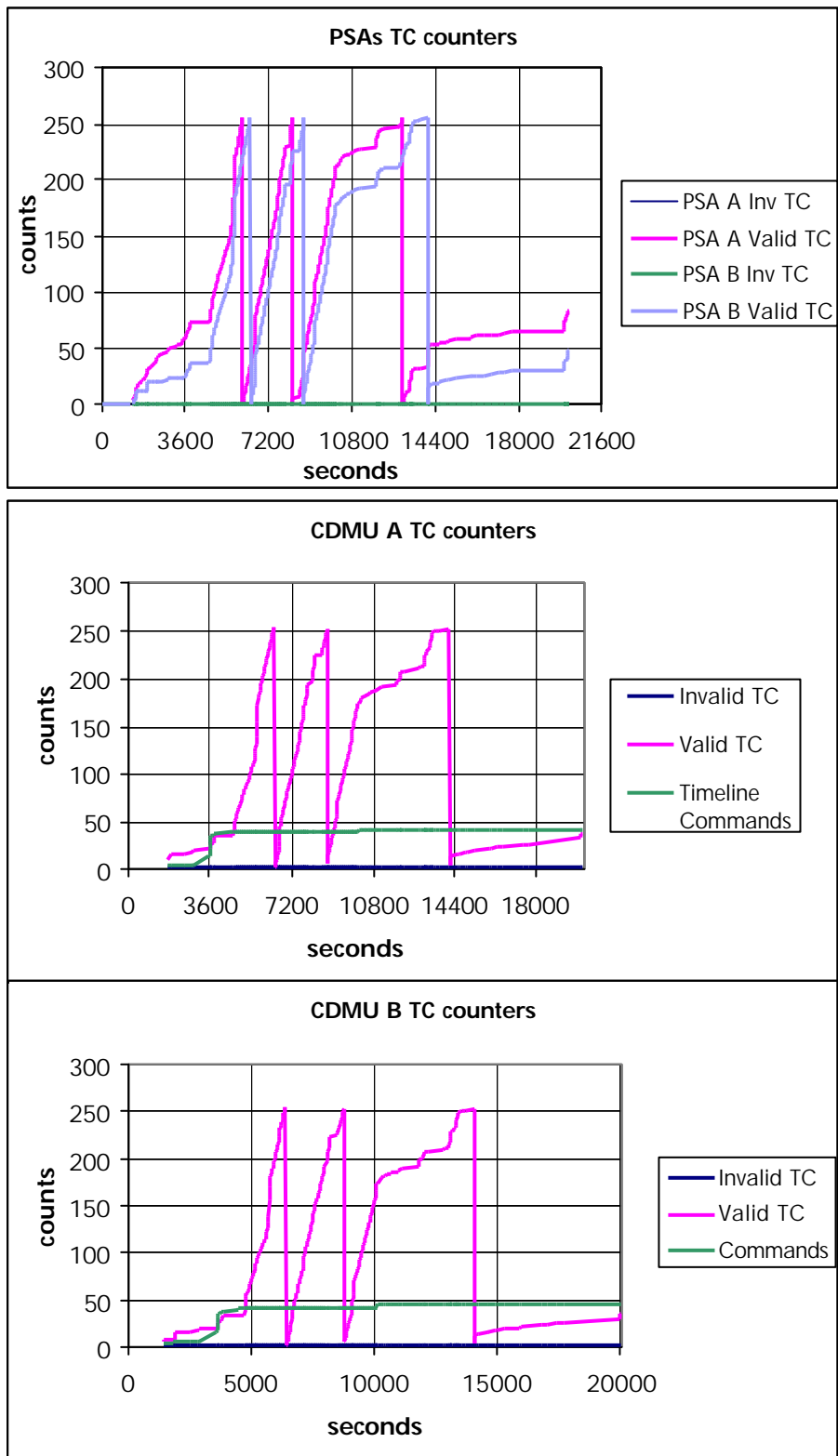


Figure 5.1-1: F14 telecommand counters telemetry

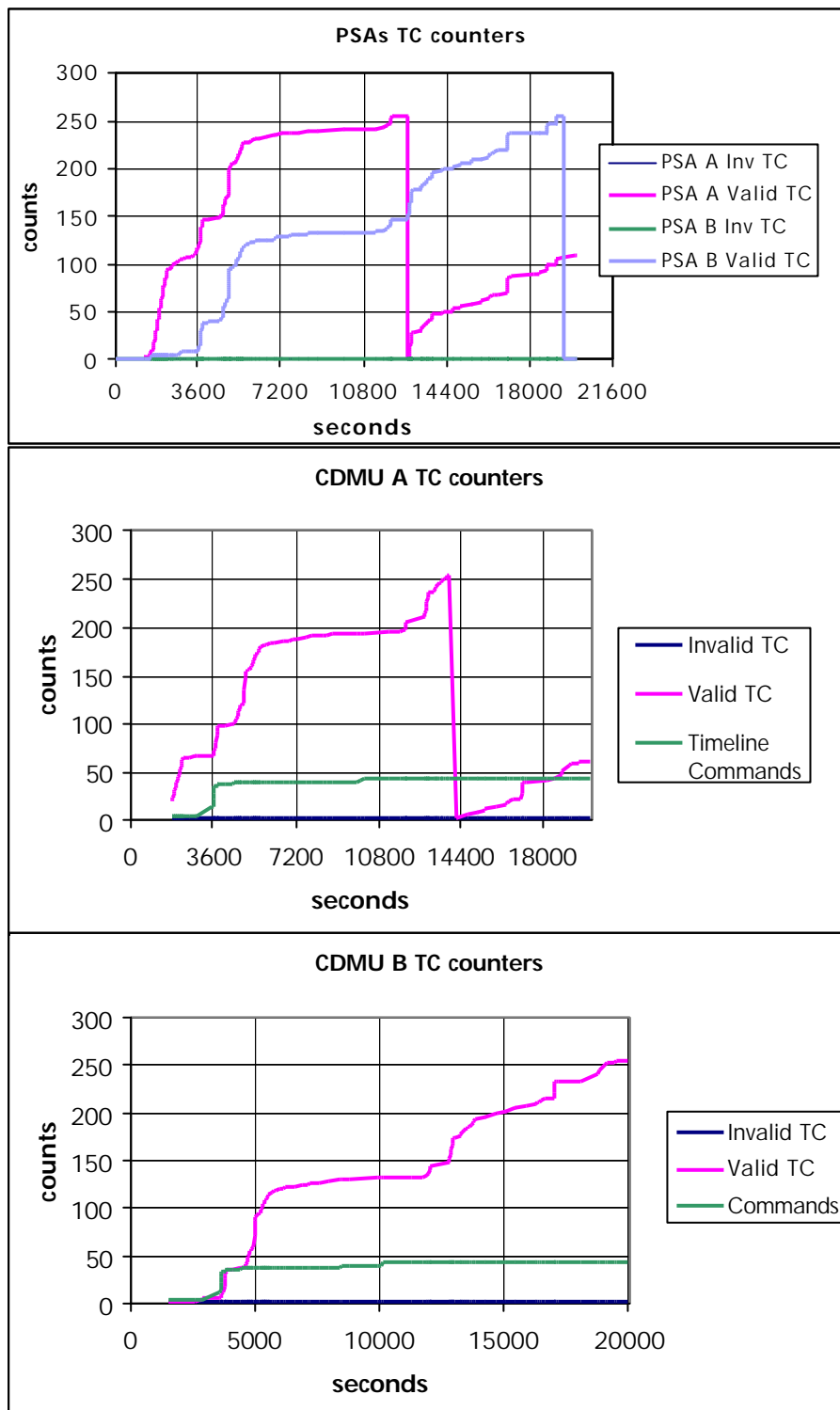


Figure 5.1-2: F15 telecommand counters telemetry

5.2 TELEMETRY FRAMES AND PACKETS STRUCTURE

This section deals with the review of the data contained in the telemetry frame and packets headers, especially the various sequence counters evolution with time.

For all checkouts, very consistent values have been observed:

- **PSA Delta Seq. Count:** A Delta value of 1 has nominally been reported on both chains.
- **PSA Delta Spacecraft Time:** A Delta value of 1 has nominally been reported on both chains.
- **Super Packets Delta Seq. Count:** A Delta value of 1 has nominally been reported on both chains.
- **Super Packets Master and Virtual Channels Frame Counts:** Periodical reset of the Master channel frame counts on both chains has nominally been noticed.
- **Dump Super Packets Delta Seq. Count and Sequence Count and Real Time Counter:** A Delta value of 1 in the sequence count and in the spacecraft time has nominally been reported on both chains. Similarly, a monotonous increase of the Dump Super Packets absolute Seq. Count has nominally been reported on both chains and the RT Count on both chains increases and resets when the probe is off.
- **Probe HK packets Delta Seq. Counts:** a Delta value of 1 has nominally been reported on both chains for HK1, 2 and 3. One Delta value of 24 has nominally been reported for HK4 on both chains: it corresponds to the reset of this HK packet (which contains entry acceleration data), 6.4 min after $T_{\text{probe ON}}$. This mechanism will permit to report the entry acceleration profile to Cassini then ground after the establishment telecommunication link, during the real mission.

Only spurious increases in the super packet delta counts before probe turn on time was reported during F5, and a telemetry retrieve problem was suspected (see RDO6). This assumption has been confirmed by ESOC and corrected. The anomaly did not reproduce during following checkouts.

5.3 TELECOMMUNICATION

Here are addressed the telemetry parameters related to the telecommunication subsystem, its units, and the DWE experiment, as acquired in the probe system housekeeping.

Main related features are:

- RF link on chain A makes use of TCXO's or TUSO/RUSO.
- Cassini HGA is pointed towards the Sun up to F4 checkout in order to shadow the

rest of the spacecraft. For the subsequent checkouts, the HGA points the Earth, and the Sun is constantly outside the HGA main lobe.

- ❑ **PSA secondary voltages:** PSA 12V, 5V and LNA supply voltage (nominally 12V), are in their nominal range and perfectly stable over all tests.
- ❑ **RUSO status:** RUSO is not switched on during F2, F6, F10 and pre-heating validation test (CO1/CO1a type). For other checkouts: RUSO is turned on 16s after PSA A is on; RUSO reports lock status at about RUSO on+16 min, well in line with expected behavior.
- ❑ **TUSO status:** TUSO is turned off by command, immediately after its automatic switch on during F2, F6, F10 and pre-heating validation test. For other checkouts: TUSO is turned on 16 s after Probe is on; TUSO reports lock status at about TUSO on+16min. The higher the temperature, the shorter the time to lock. Note that the mission timeline, after the implementation of the probe pre-heating strategy, will permit during mission warm up duration as long as 4h30min instead of 30 min.
- ❑ **TCXO's status:** TM nominally reports TCXO selection on chains A & B during F2, F6, F10 and pre-heating validation test, TM nominally reports TCXO selection on chain B and not on chain A for other checkouts.
- ❑ **HPA/TX power:** For all checkouts, as expected, HPA is off, and no power is monitored at TX output. **Note that flight spare HPA's were turned ON on the EM Probe, and operated properly, after 6 years in OFF state.**
- ❑ **Receiver's status:** For all checkouts, TM nominally reflects on both chains a RSW state of 2 until the TX's are turned on.

As expected, switch to basic frequency happened successfully at the first attempt for chains A and B, when both of them operating on TCXO (F2, F6, F10 and pre-heating validation test).

For the other checkouts:

- on chain A when operating with TUSO/RUSO, state 6 (carrier, subcarrier, bit sync and Sync Marker locked) has been reached after the 5th, the 6th and the 7th attempt depending the checkout (it shall be noticed that F1 showed a complete receiver lock on chain A during CO2 at the 3rd attempt; and on ground at worst, lock was achieved at the 2nd attempt). As noted from F4, this is not a concern (in total the sequence plans 28 attempts to switch to basic frequency) and this phenomenon is related to the initial temperature of TUSO. A colder temperature leads to a longer time for the TUSO oscillator frequency to stabilize and enter in the 30kHz PSA acquisition bandwidth. It should be pointed out that this problem will not happen during the mission: about 4h30min TUSO warm up time is foreseen before PSA attempts to acquire the probe RF signal in basic frequency mode (as in checkout because of the Cassini-Huygens geometry change in the frame of the Recovery Mission). At that time, the frequency variation of the transmitted signal will be far below the requested 30kHz.

- on chain B (no TUSO/RUSO), switch to basic frequency is successful at the 1st attempt.
- **AGC:** Anomalies have been identified during F1 and F2 checkouts :
- during F1, a loss of some 4.5dB compared to the expected value has been noticed on both chains. In addition, an abnormal evolution in the course of the checkout has been flagged with changes of some 2dB.
 - during F2, further losses of 3dB (chain A) and 5.4dB (chain B) wrt F1 have been identified with a still abnormal evolution of the signal during the checkout.

After a dedicated investigation, it was proved that the reported AGC variations are correlated with the Cassini HGA pointing at the Sun and that the signal drop was due to the Sun RF noise injected at the input of the receiver. This configuration was specific to F1 and F2 because of the necessary use of the HGA as thermal shield. It did not reproduce for subsequent checkouts.

The AGC history in Figure 5.3-1 hereunder evidences the AGC evolution since the first flight checkout. The AGC levels from F3 are well in accordance with conclusions reached after the AGC specific test (see RDO3): the favorable AGC level is explained by the Earth-spacecraft-Sun geometry considering that from F3, the HGA was pointed towards the Earth, and then by the increasing spacecraft-Sun distance.

A simultaneous drop in the AGC values on both chains by 0.2dB about 40min before the end of the F11 test was also noticed. No convincing correlation has been found with on board events, but, however, this issue was considered as a minor observation as far as the probe system is concerned.

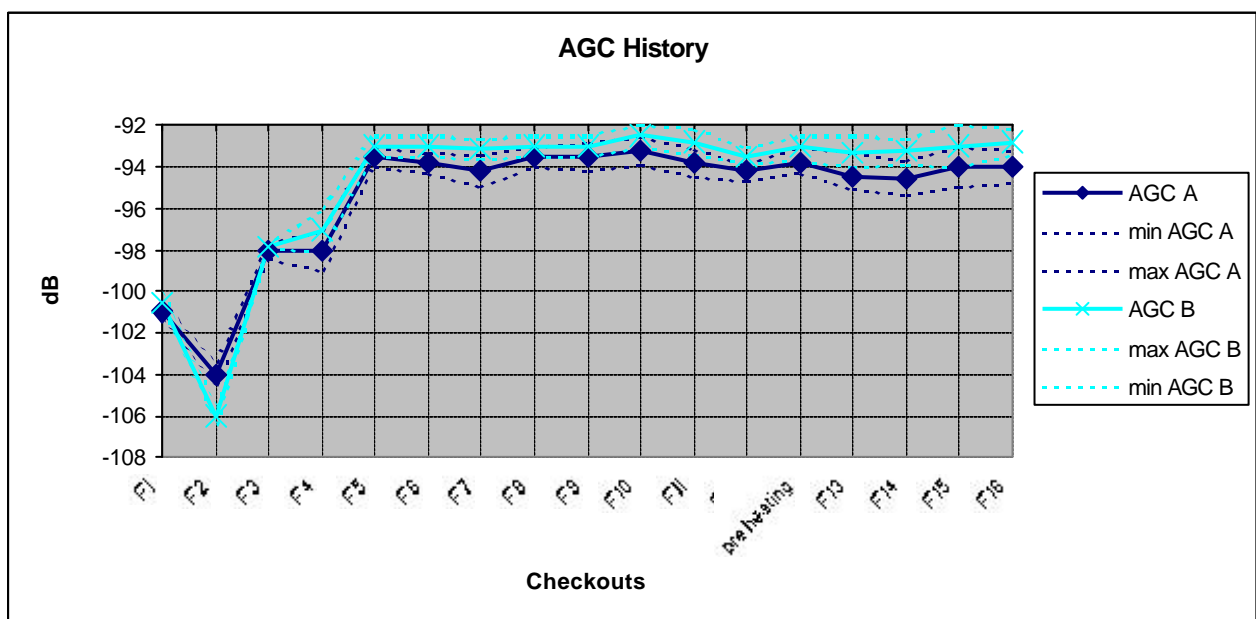


Figure 5.3-1: AGC history

- **NCO:** As far as the probe system is concerned, NCO frequency changes were as expected, both on chain A (TCXO or RUSO) and chain B (TCXO), and very similar. It shall be underlined that the NCO frequency modulation noticed by DWE, observed during F1, F3, F4, F5, F7, F8, F9, F11, F12, F13, F14, F15, F16 (~0.367Hz with a maximum amplitude oscillation of about 20Hz, see DWE checkout reports) is currently not a probe system concern. Also, so-called dF/dt parameters on both chains were within the expected range for all checkouts.

5.4 POWER

This chapter will first address the periodic checkouts, under the perspective of the power subsystem, the battery depassivation sequence 1 which has occurred few days after F15, and the battery depassivation sequence 2.

5.4.1 Checkouts

- **Cassini Telemetry** has shown :
 - PSA A average consumption is 25W with RUSO off, ranges from 40W during RUSO warm up phase, down to 32W afterwards with RUSO on
 - PSA B average consumption is 25W, which means a total PSE steady state consumption of 50W, for the checkouts run with RUSO off, and of 57W for the checkouts run with RUSO on
 - Probe total average maximum consumption is 150W.

These values are well in line with expected results.

- **Current limiters status and pyro relays status** have been cross checked with the retrieved telemetry :
 - Nominal current limiter status changes during all checkouts are fully in line with the Mission Timeline and checkout sequencing. Figures 5.4-1 and 5.4-2 show the nominal current limiters changes along F14 and F15 (S₀ happens at 3600s).
- For all checkouts, all the nominal and redundant pyros selection relays were set and reset by each of the chains at the expected time wrt the Mission Timeline Table. The Figure 5.4-3 illustrates the relay status changes during checkouts. It shall be noted that the period of reporting of the pyro selection relay status is 16s.

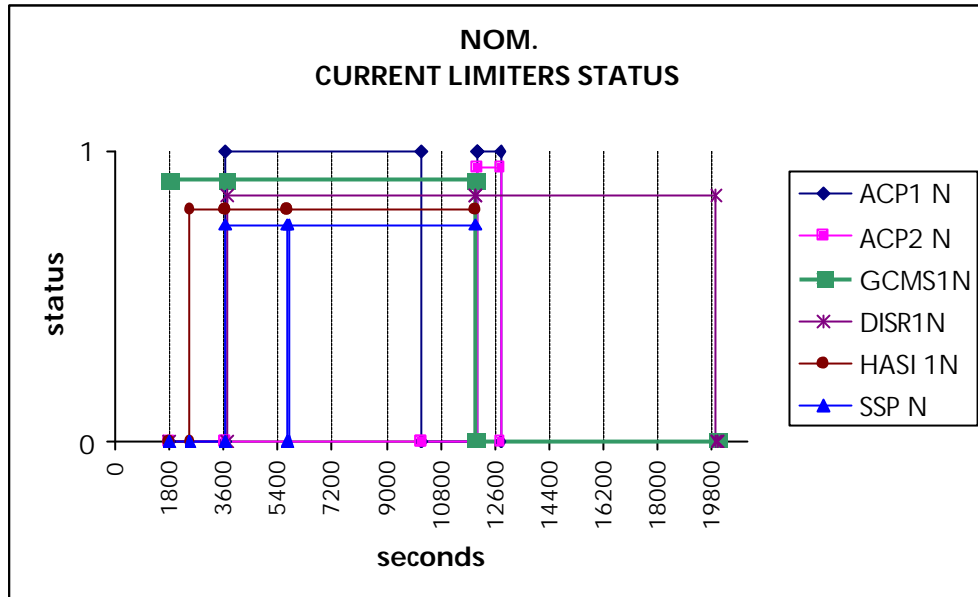


Figure 5.4-1: Nominal current limiters status changes along F14 ("0" = start of F14)

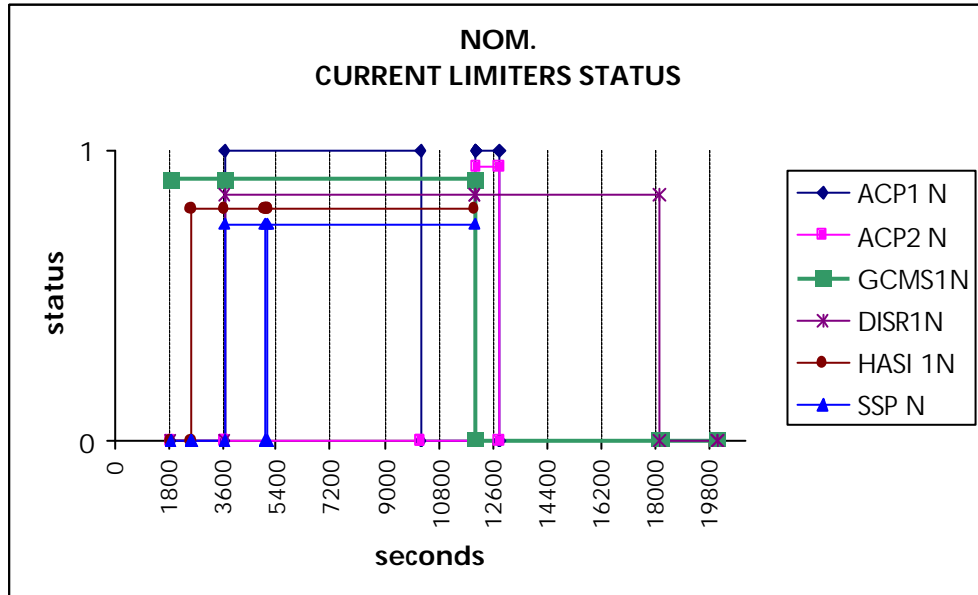


Figure 5.4-2: Nominal current limiters status changes along F15 ("0" = start of F15)

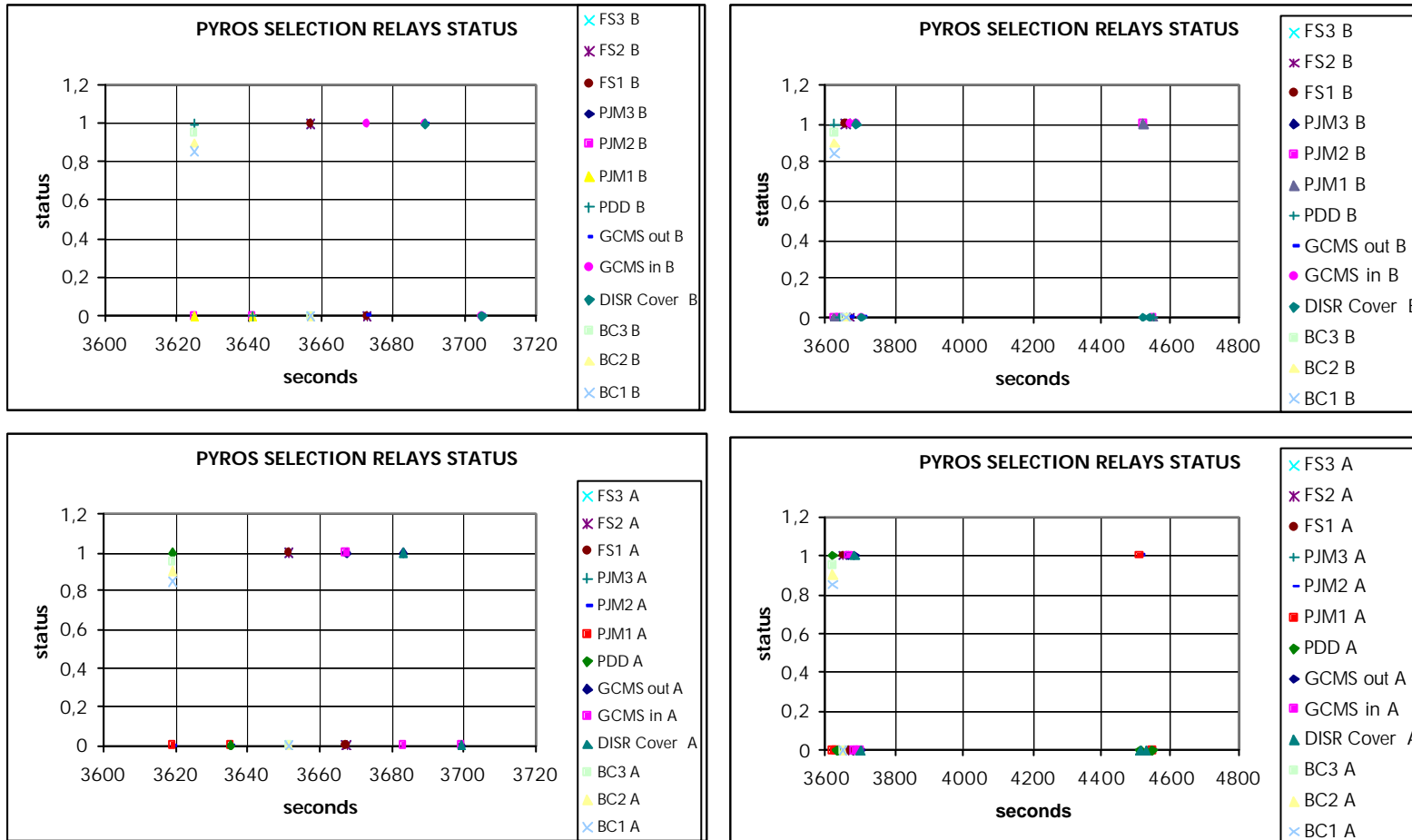


Figure 5.4-3: Reported selection relay status changes during checkouts (NB: S_0 is at $t=3600s$)

- **Main bus voltage** is 28.09 Volt, as expected, for all the checkouts.
- **Battery voltage** telemetry at the end of the tests is gathered in the Table 5.4-1 for all checkouts.

	F1	F2	F3	F4	F5	F6	F7	F8	F9	F10	F11	F12	F13	F14	F15	F16
1 A	2.93	2.28	2.00	2.6	2.00	2.28	2.6	2.6	2.6	2.6	2.93	2,93	4,89	4.24	3.26	2.93
2 A	2.6	2.28	2.00	2.28	2.00	1.96	2.28	2.6	2.6	2.6	2.93	2,93	4.56	3.91	2.93	2.93
3 A	1.3	1.30	1.00	1.30	1.00	0.98	1.30	1.30	1.30	1.30	1.63	1.63	2.6	1.96	1.63	1.63
3 B	1.3	1.30	1.00	1.30	1.00	0.98	1.30	1.30	1.30	1.30	1.63	1.63	2.6	2.28	1.63	1.63
4 B	2.6	2.28	2.00	2.30	2.00	1.96	2.28	2.6	2.6	2.6	2.93	2,93	4.56	3.91	2.93	2.93
5 B	2.28	1.96	1.63	1.96	1.63	1.63	2.28	2.28	2.28	2.28	2.6	2.6	4.24	3.59	2.6	2.6

Table 5.4-1: Battery voltage at the end of checkouts

Note that these voltages, as long as batteries are not connected to the PCDU (ie for all checkouts except depassivation) are not in any way representative of the actual battery voltages. They reflect the leakage current in the telemetry measurement diode, which is somewhat proportional to the PCDU temperature: the voltages are, indeed, fully consistent with the PCDU final temperature, as addressed in section 5.7.

The lower battery 3 voltage parameter is due to the cross trapping of the relevant telemetry measurement electronics.

- **BDR currents** are in accordance with the operating modes of the probe system and experiments for all checkouts. Average F11 BDR currents over typical time periods are given in the Table 5.4-2.

	Pre To	To to To +110 mn	to To+140 mn	to To+156 mn	to To+227 mn	to To+274 mn
BDR1	0,55 A	0,82 A	0,82 A	0,58 A	0,45 A	0,37 A
BDR2	0,49 A	0,72 A	0,72 A	0,51 A	0,4 A	0,33 A
BDR3	0,49 A	0,72 A	0,72 A	0,51 A	0,4 A	0,33 A
BDR4	0,49 A	0,72 A	0,72 A	0,51 A	0,4 A	0,33 A
BDR5	0,55 A	0,82 A	0,82 A	0,58 A	0,45 A	0,38 A
BDR 1&5 vs BDR 2,3&4 balancing	1,12	1,14	1,14	1,14	1,13	1,15

Table 5.4-2: BDR currents during F11 checkout

The unbalancing of the BDR's 1 and 5 is nominal (spec is 1.14+/-5%), set to compensate the batteries 2, 3 and 4 discharge during the coast phase when supplying the Mission Timer Unit (MTU).

- **currents** (mean values) are summarized in the Table 5.4-3. They are in perfect accordance with the expected loads during checkouts, which partly consolidates the power and energy budgeted for the mission (not all the loads can be connected during checkouts).

UNITS	CURRENT (A)	UNITS	CURRENT (A)
TX A	0.19	TX B	0.195 A
TUSO N off	0	TUSO R off	0 A
TUSO N on	0.32 warm up 0.127 steady state	TUSO R on	0.3 A warm up 0.120 A steady state
CDMU A	0.326	CDMU B	0.337 A
Prox Sensor A	0	Prox Sensor R	0 (unit is OFF)
DISR1 N	0.16 /peak 0.25	DISR1 R	0.15 A/peak 0.25 A
DISR2 N	0	DISR2 R	0
GCMS1 N	in pre To 0.28 (F1, F3, F4, F5, F7, F8, F9) 0.25 (F2, F6, F10, F11) in post To 0.38 (F1, F3) 0.4 (F4, F5, F7, F8, F9) 0.42 (F2, F6, F10 to F16) HP Mode 0.58 (F1) 0.6 (F3, F5, F7)	GCMS1 R	in pre To 0.26 (F1, F3, F4, F5, F7, F8, F9) 0.23 (F2, F6) 0.24 (F10, F11) in post To 0.36 (F1, F3) 0.38 (F4, F5, F7, F8, F9) 0.4 (F2, F6) 0.39 (F10 to F16) HP Mode 0.55 (F1, F2) 0.65 (F3) 0.6 (F5, F7)
GCMS2 N	0	GCMS2 R	0
HASI1 N	0.2 in post To	HASI1 R	0.18 in post To
HASI2 N	0	HASI2 R	0
ACP1 N	0.07	ACP1 R	0.07
ACP2 N	0	ACP2 R	0
ACP3 N	Peaks up to 0.35 (0.8, F4)	ACP3 R	Peaks up to 0.38 (0.95, F4)
SSP N	0.32 (F1 to F9) 0.33 (F10 to F16)	SSP R	0.027 (F1 to F9) 0.03 (F10 to F16)

Table 5.4-3: Unit and instrument currents during checkouts

5.4.2 Depassivation

1st depassivation sequence

The first depassivation sequence was run 5 days after F15. Its purpose was essentially to get an early feeling on the flight batteries status, considering that this had become the main driver for the pre heating – no pre heating decision. The whole sequence was reassessed and slightly adapted to take into account the current units power consumption. As a reminder the depassivation sequence consists in applying a constant, defined load (typically 1A) during 5mn to each of the batteries, one by one., in order to “break” the passivation layer of the Lithium electrode. The power loads are constituted by the Probe units and experiments.

The results of the test are expressed in figures 5.4-4, 5.4-5, 5.4-6, 5.4-7.

They show that the sequence has been nominally executed, and that each of the battery voltage was around 70V (Figure 5.4-7) in the conditions of the test (batteries temp is displayed in Fig. 5.4-8). This indicates that all the cells are in good operation, with some 2.69V/cell. This is perfectly consistent with the mean cell voltage figure of 2.65V/cell given by the manufacturer. As it appears from Fig 5.4-4, each of the batteries has been able to deliver the requested current, without any anomaly. The BDR's 1 & 5 vs BDR's 2, 3, 4 balancing is shown in Fig 5.4-5 where relevant (ie. when the BDR's 1 or 5 were in use with the BDR's 2, 3 or 4); the values are perfectly consistent with the expected 1.14 +/-5%.

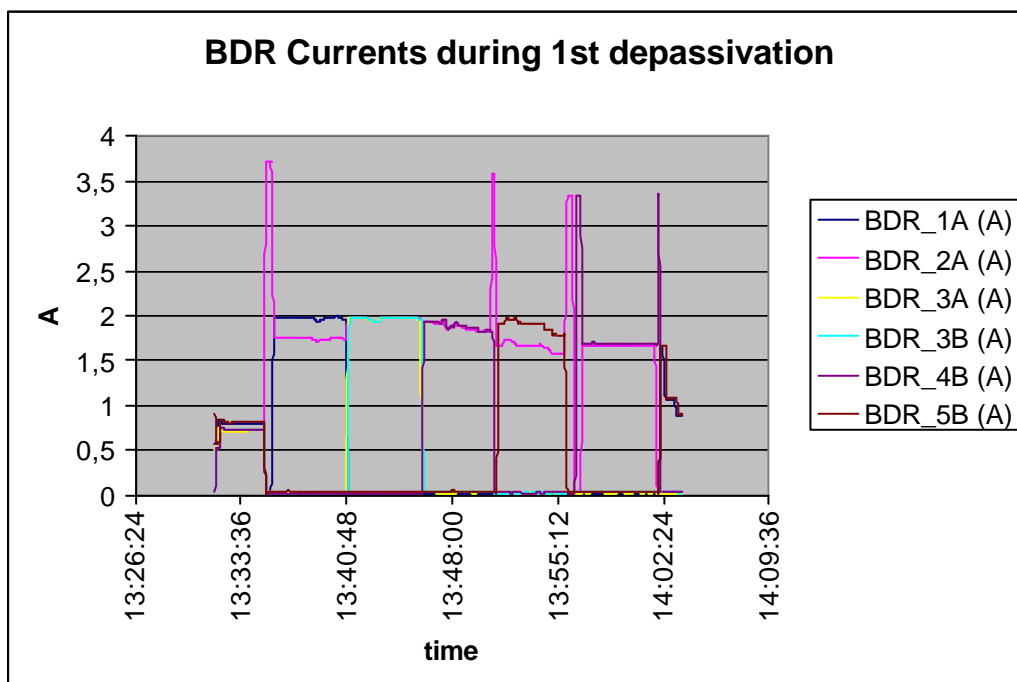


Figure 5.4-4: BDR currents for 1st depassivation sequence

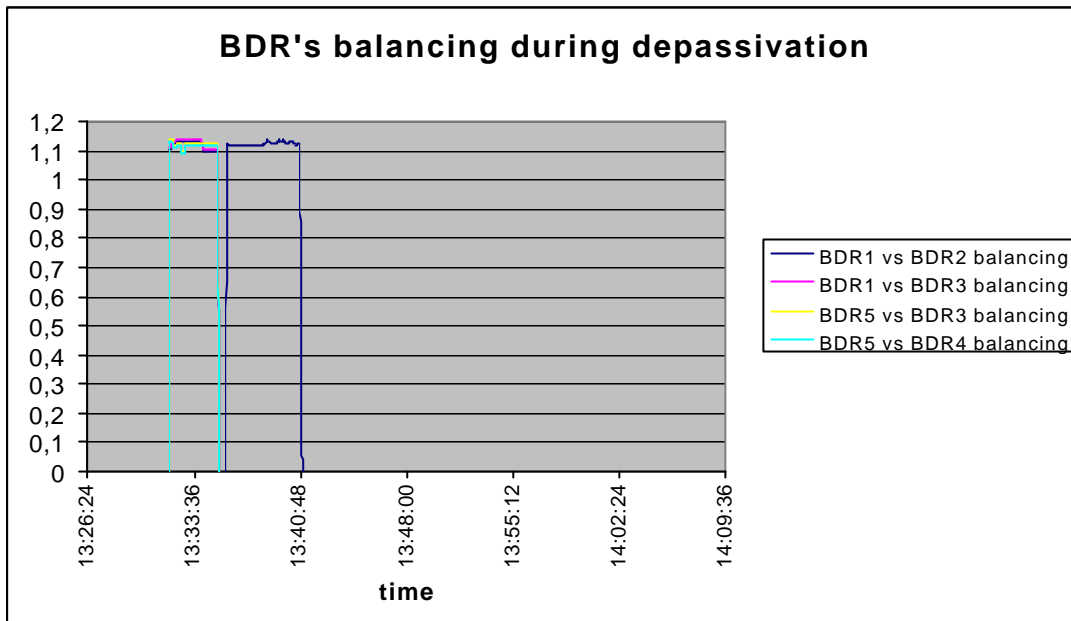


Figure 5.4-5: BDR currents **balancing** for 1st depassivation sequence

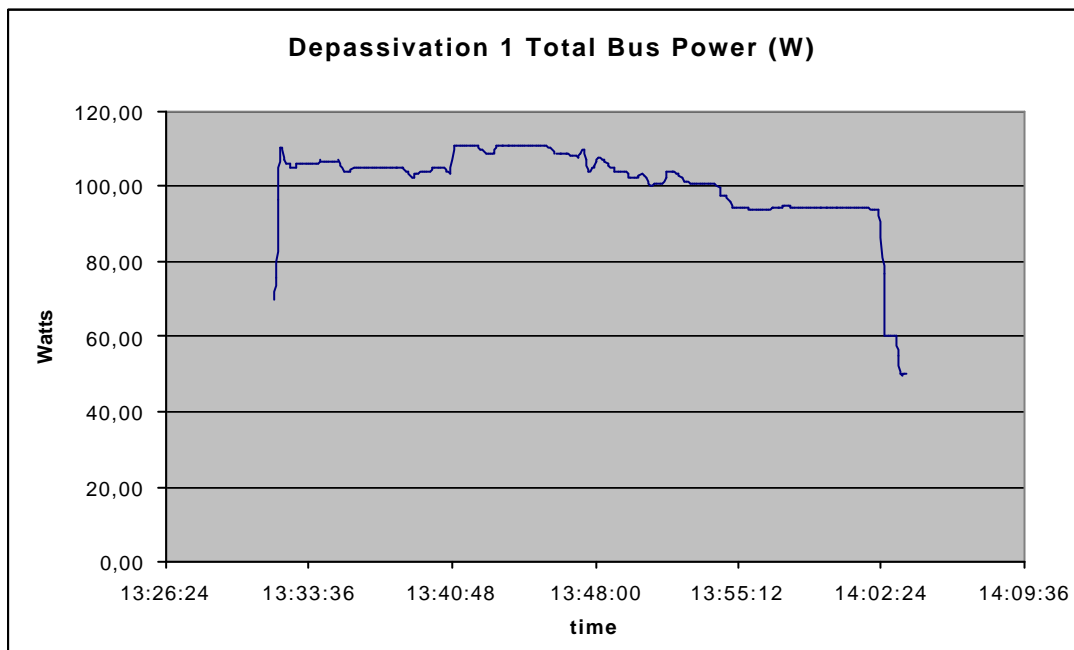


Figure 5.4-6: Total Bus power demand for 1st depassivation sequence

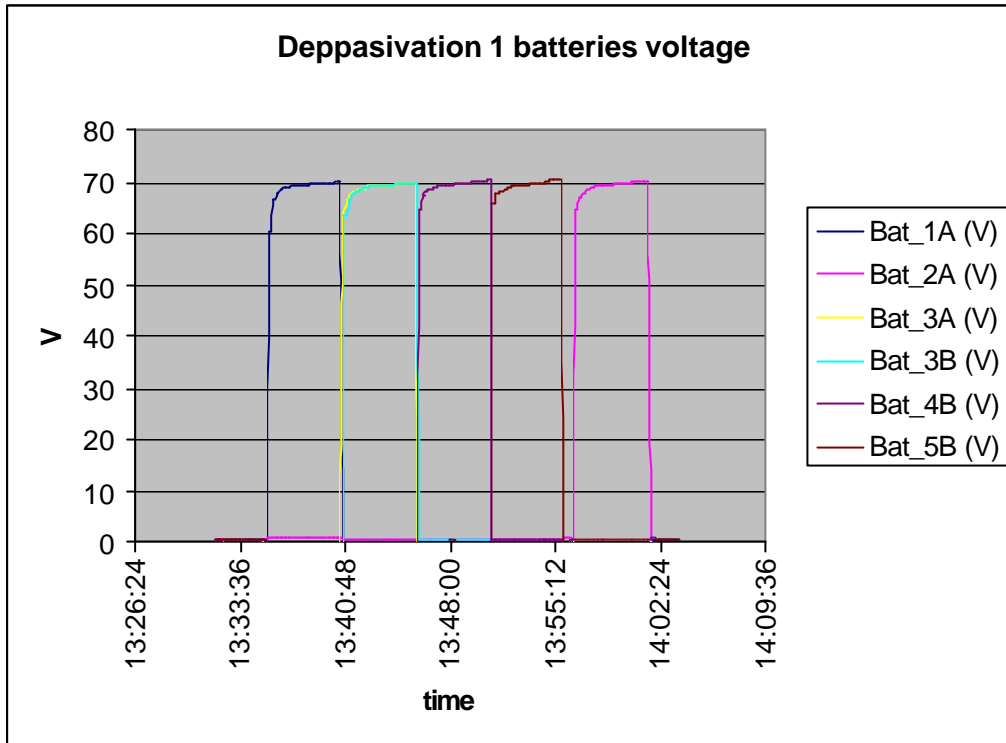


Figure 5.4-7: Battery voltages during 1st depassivation sequence

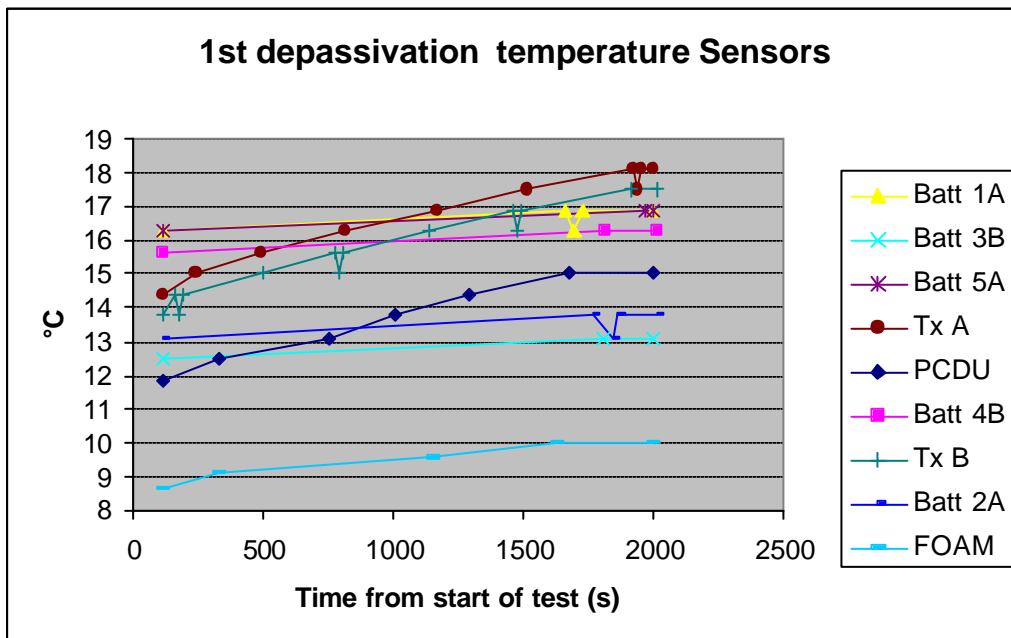


Figure 5.4-8: Temperatures during 1st depassivation sequence

2nd depassivation sequence

The second depassivation sequence was run 12 days after F16, on the 5/12/04. It consisted in the nominal batteries depassivation and had essentially 2 objectives :

- to be a go-nogo criterion for the implementation of the Probe pre heating option
- to be a go-nogo criterion for the nominal Probe mission during descent.

The Sequence was identical to the 1st depassivation sequence.

The results of the test are expressed in figures 5.4-9, 5.4-10, 5.4-11, 5.4-12. As support of the analysis, Figure 5.4-13 displays the temperatures reached by the batteries and PCDU.

These show that the sequence has been nominally executed, and that each of the battery voltage were around 70V (Figure 5.4-12) in the conditions of the test. All the cells status appear nominal, with some 2.69V/cell, as for the depassivation#1, consistent with the mean cell voltage figure of 2.65V/cell given by the manufacturer. Some minor differences can be seen compared to Fig 5.4-7 : the initial batteries voltage was slightly lower than during the 1st depassivation. This behaviour is fully in line with the fact that the batteries temperature during the 1st depassivation has been $\sim +4^{\circ}\text{C}$ higher than during the 2nd depassivation.

Fig 5.4-9 demonstrates that each of the batteries was able to deliver the requested current, without any anomaly. The BDR's 1 & 5 vs BDR's 2, 3, 4 balancing is shown in Fig 5.4-10 where relevant (i.e. when the BDR's 1 or 5 were in use with the BDR's 2, 3 or 4); the values are perfectly consistent with the expected $1.14 \pm 5\%$, and with the 1st depassivation results.

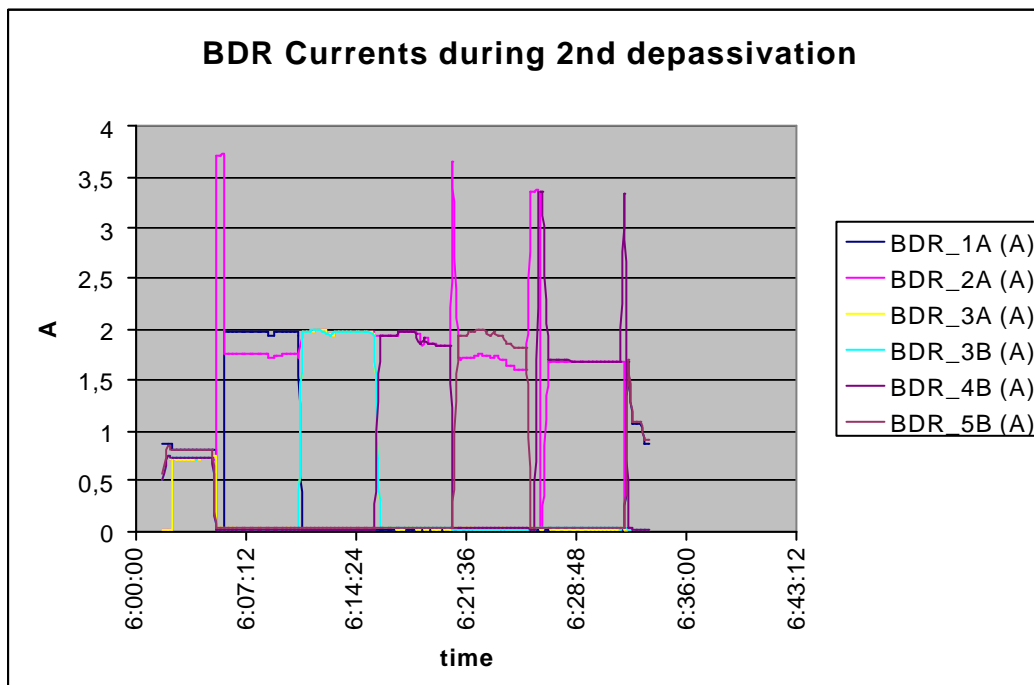


Figure 5.4-9: BDR currents for 2nd depassivation sequence

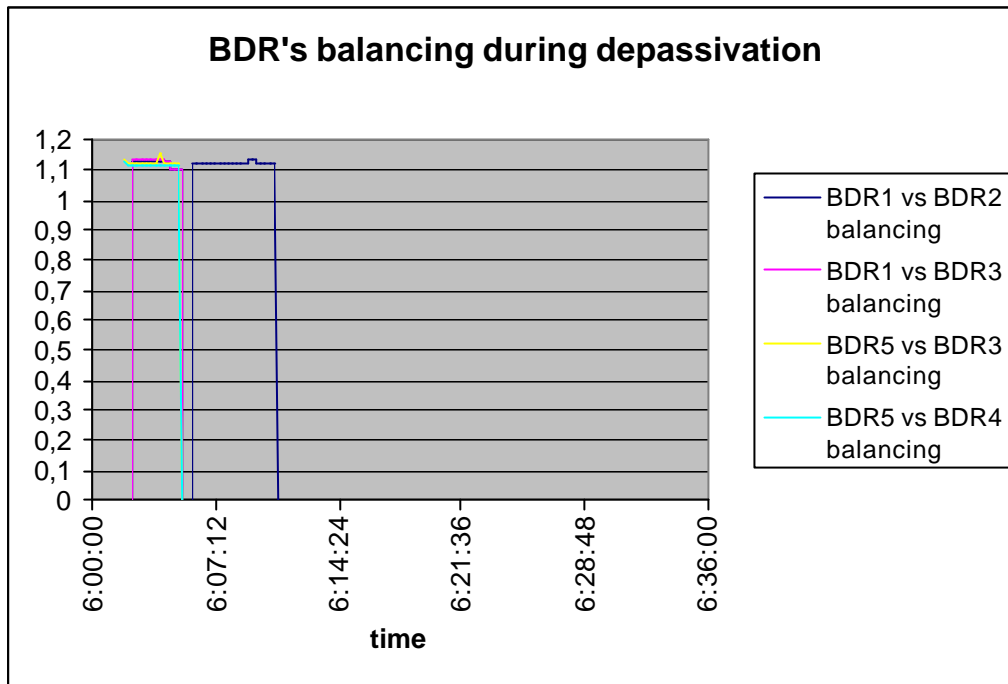


Figure 5.4-10: BDR currents balancing for 2nd depassivation sequence

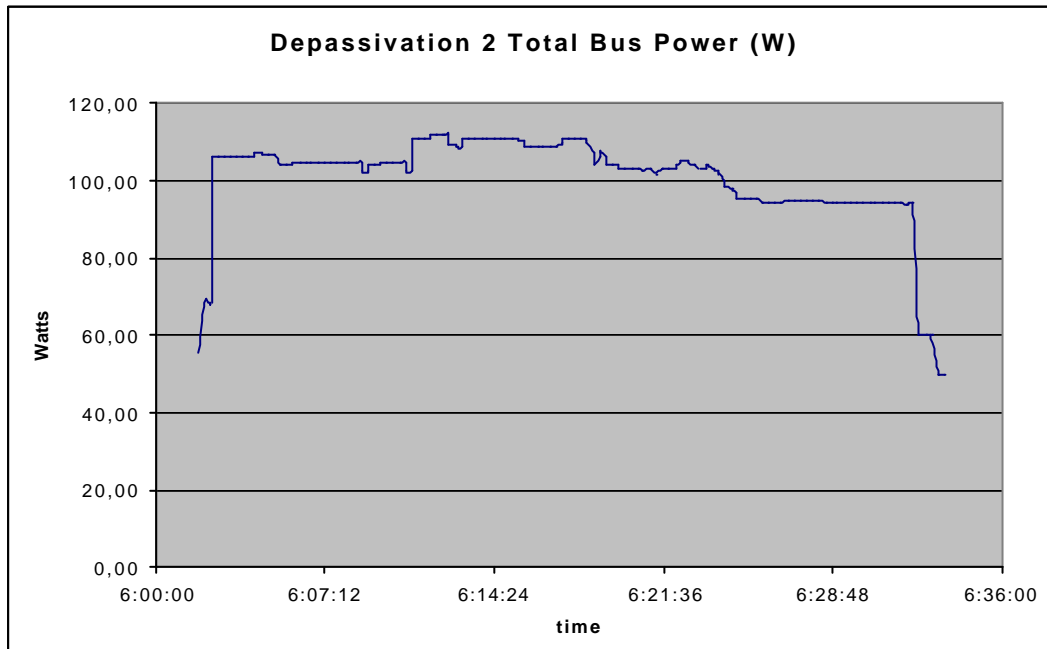


Figure 5.4-11: Total Bus power demand for 2nd depassivation sequence

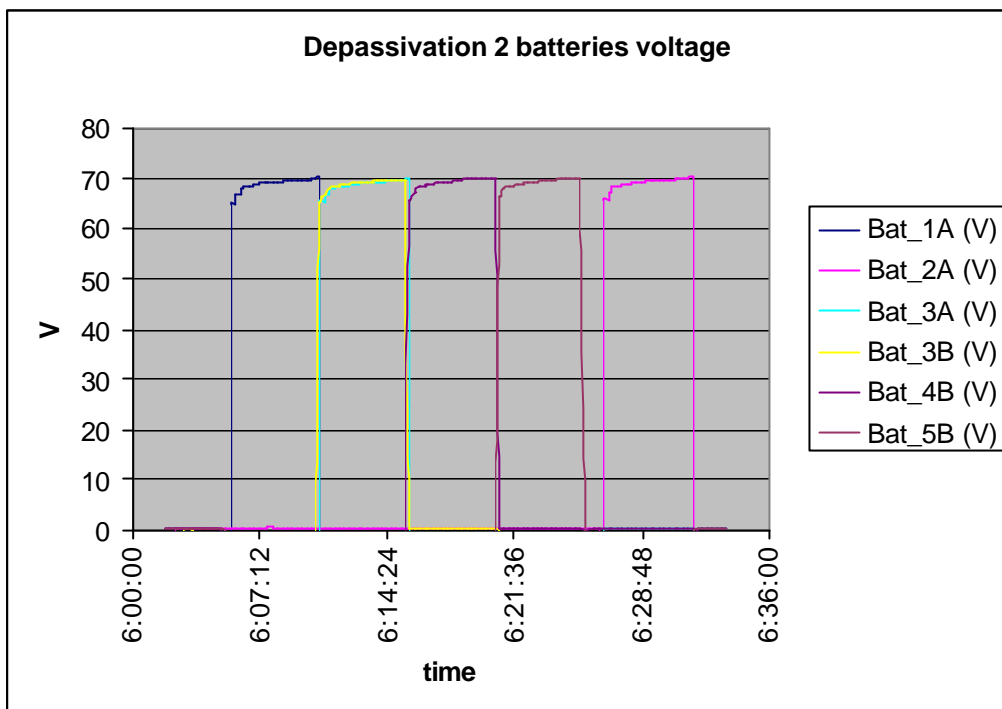


Figure 5.4-12: Battery voltages during 2nd depassivation sequence

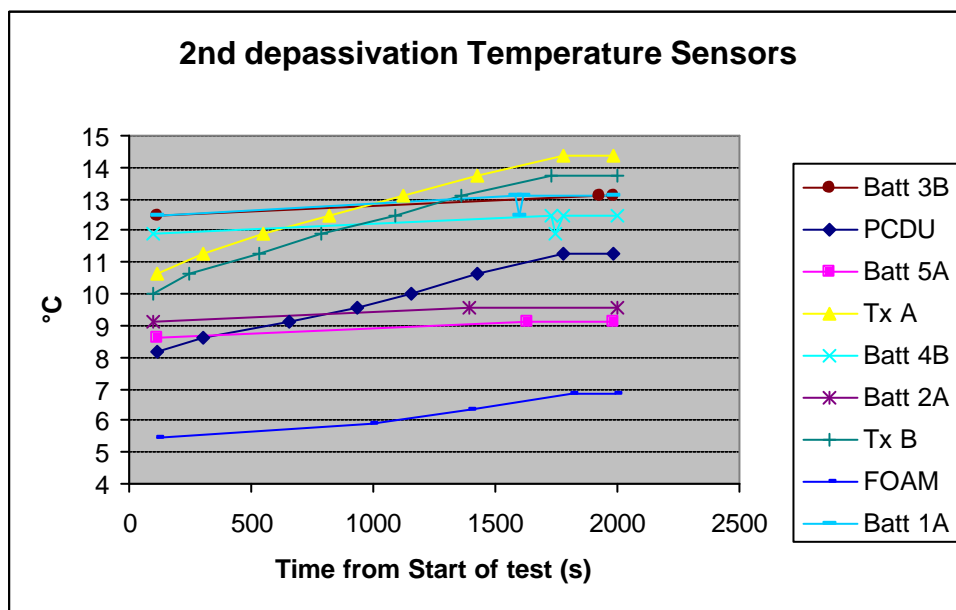


Figure 5.4-13: Temperatures during 2nd depassivation sequence

5.5 DATA HANDLING

This section deals with the analysis of all the telemetry data related to the CDMS, and to the PSA's data handling functions.

- **Central Acceleration data:** The expected TM reported on A and B is 0 g for the accelerometer 1 (parameters 1A, 1B) accelerometer 2 (parameters 2A, 2B) and 3 (parameters 3A, 3B).

Spurious drifts on the accelerometers 1 and 3 telemetry were evidenced during F1, F2, F3 and F4. While the noise peaks reported within F1 and F2 were marginal, the problem got much worse during F3 with noise peaks reaching up to 2 LSBs, then slightly reduced during F4.

The situation during F5, F6, F7 and F8 improved again: only accelerometer 1 TM seldom showed 1 LSB peaks. F9 was in line with these measurements, marginally degraded wrt F8. F10 was in line with F9. F11 showed an apparent return to fully nominal conditions.

Spurious drifts on the accelerometer 1 and significant 3 LSB noise peaks on the accelerometer 3 during F13 (see Fig 5.5-1) and on accelerometer 2 during F14 were again reported in the telemetry, while the situation was improved for accelerometers 2 and 3 during F15. Finally F16 exhibited even fewer spurious noise on any of the accelerometers.

Figure 5.5-2 summarizes the overall CASU behavior by showing the "CASU LSB noise" history; the number of "LSB counts" is cumulated for each checkout and each accelerometer.

Tentative explanations for the spurious acceleration values were provided in the F3 report, giving as a possible explanation a stiction effect at the level of the accelerometers 1 and 3. This is actually not in contradiction with the observed improvement in F11 for instance, the stiction being strongly dependent upon the initial conditions of the test. It shall also be noticed that the stiction (dry friction) phenomenon may apply on both positive and negative directions. The fact that no spurious appears from accelerometers 1, 2 and 3 during F11 could thus reflect a negative shift of these sensors, not visible because the negative values are "cut" by the TM acquisition electronics.

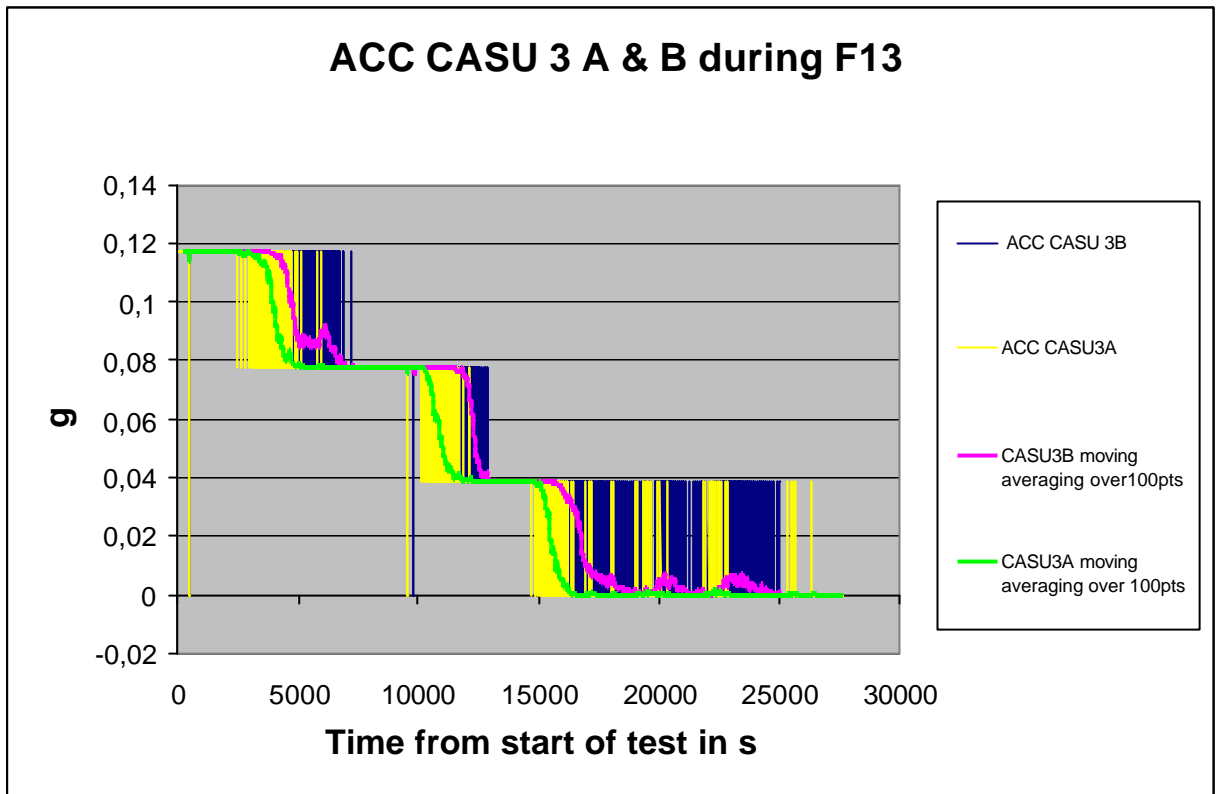


Figure 5.5-1 CASU ACC 3 measure during F13

The assessment of the CASU accelerometers anomaly consequences, detailed in RD14, has shown that it was not leading, even in worst case (3 LSB offset) to violation of entry conditions constraints. This has justified a "use as is" statement.

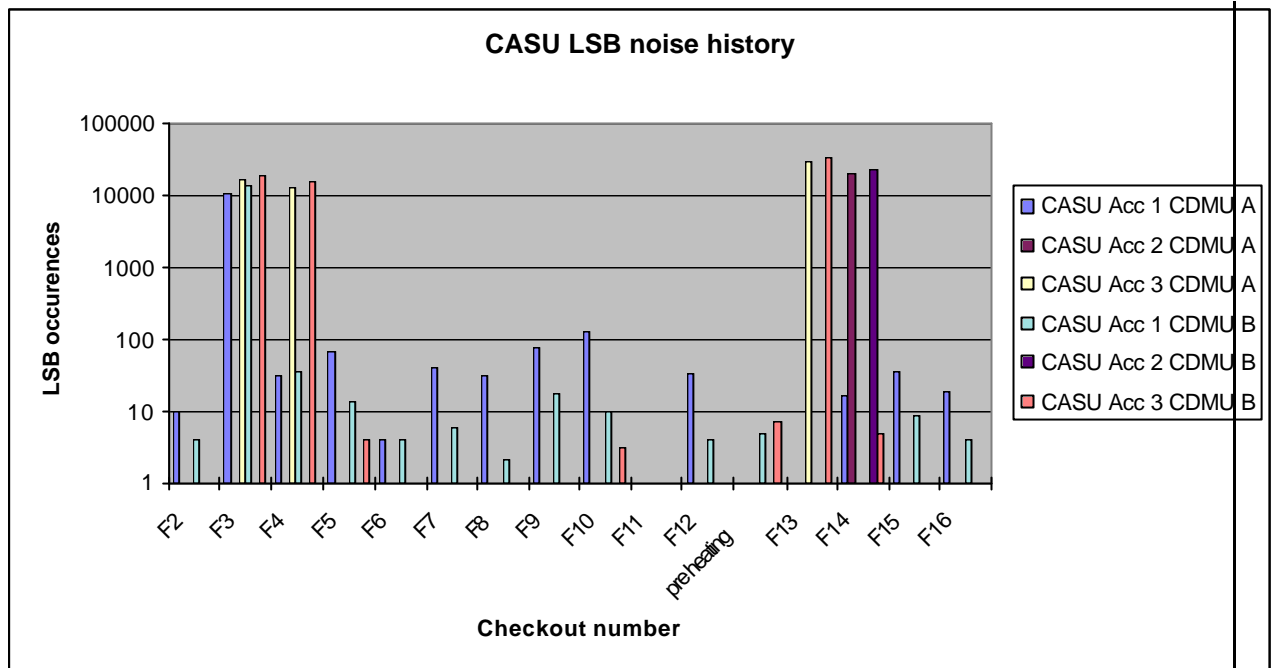


Figure 5.5-2 CASU noise history

- **Radial Acceleration data:** The reported TM nominally showed a 0-g value for all checkouts.
- **DDB Mission Phase flags:** The telemetry properly reported the mission modes changes: mission modes switch between Flight Checkout, Flight Checkout Suspended and De-activate modes following checkout sequence.
- **DDB F1 & F2 flags status:** To "detection" was correctly reported on both chains through F1 change. F2 nominally reports the Time Altitude Table (TAT) use over the whole sequence. Note that To corresponds to the time of pilot chute firing, and $T_o = S_o + 6.375s$ where S_o corresponds to the g-threshold detection by the POSW.
- **DDB Time:** For both chains, it was in line with Probe Real Time before T_o , then with Probe [Mission Time - 6.375s] from T_o to probe off.
- **DDB Altitude:** Nominally set to 320 km until T_o , then followed the TAT down to "surface" (Proximity Sensor is off).
- **DDB Spin:** TM reported the spin profile simulated via the CO1 test sequence (alteration TC's). TM reported permanently Orpm since spin is not simulated when CO2 type sequences.
- **μprocessor Valid:** As expected and depending on related checkout, the analysis of the Probe status showed that both CDMU's have been set as " valid " all along tests

duration, giving the experiments the opportunity to listen to the chain A (CO1), or as " invalid " from Tp+ 35min, giving the experiments the opportunity to listen the chain B (CO2). Processor valid evolution for the different checkouts is shown in Figures 5.5-3 and 5.5-4 hereafter.

- **MTU:** All three timers registers content, as read by both CDMU's, were reported to be 16#FFFF. These are the expected values when the MTU is turned on, but not programmed, as per all checkouts from F1 to F16.

The MTU drift tests run within F13 and F14 slots have shown a nominal MTU countdown in line with the value programmed from both CDMU A and B before formal checkout start. F14 slot test was specifically designed to get accurate measurements of flight MTU oscillators stability and has demonstrated for each of the 3 MTU timers, drift lower than 1 minute (55 to 57.5s) in 22 days, consistent with the allocation and the entry time uncertainty budget.

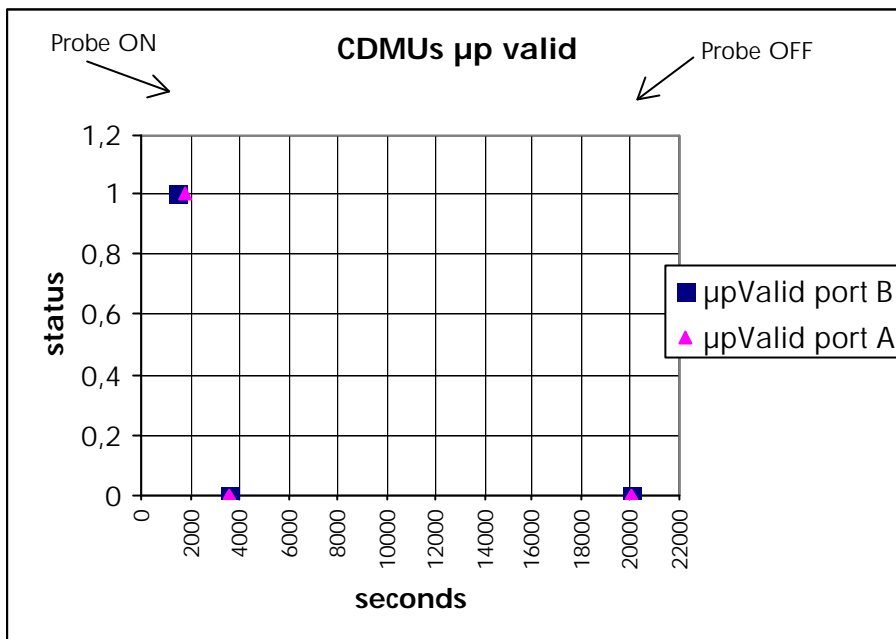


Figure 5.5-3: μ p Valid changes along F1, F3, F5, F7, F9, F11 checkouts (S0 is at t=3600s)

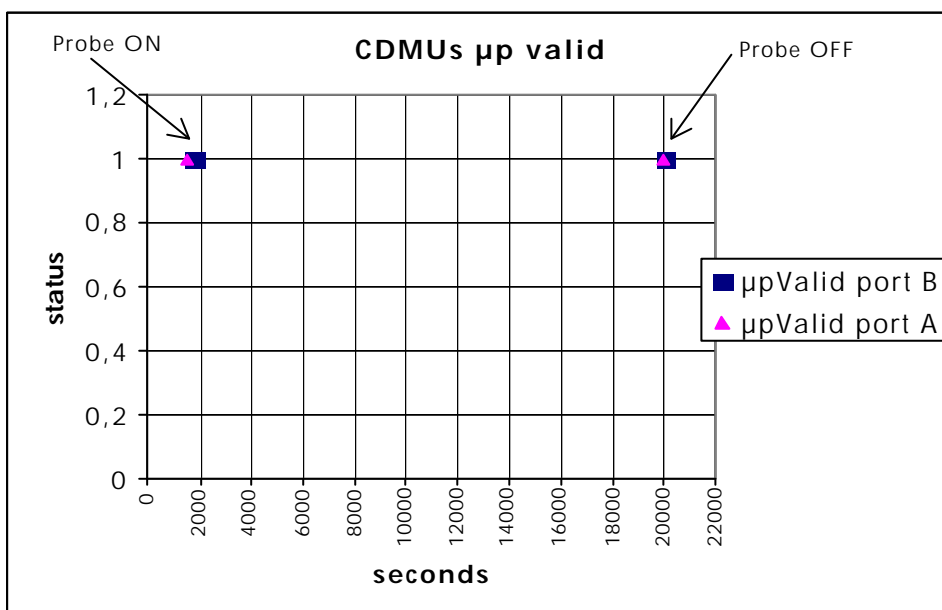


Figure 5.5-4: μ p Valid changes along F2, F4, F6, F8, F10, F12, F13, F14, F15, F16 checkouts (S0 is at t=3600s)

The MTU redundant loading sequence run during F15 and F16 slots has shown a nominal MTU loading from CDMU A and B and countdown of the three timers in line with the value programmed, as illustrated on Figure 5.5-5 for F15 and chain A (F16 is identical). Note that the 2 first increments are nominally spaced by 16s, instead of 32s for the other increments.

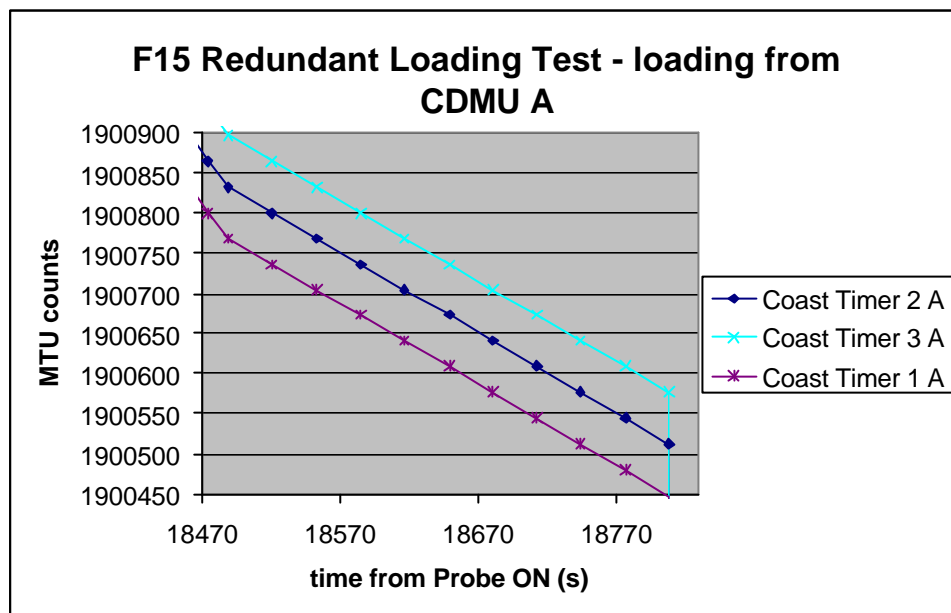


Figure 5.5-5: MTU countdown during F15 from CDMU A loading

- **EEPROM's:** For all checkouts, a complete CDMU's EEPROM (16kW) and PSA's EEPROM (8kW) dump was performed, and the content was compared to the expected one. No difference was noticed for all 4 memory banks, showing a good immunity of the CDMU's and PSA's EEPROM chips to Single Event Upsets in unbiased conditions.
- **Processor boards:** No anomaly in the PSA's and CDMU's init was noticed. In addition, no double nor single RAM (CDMU's or PSA's) error was flagged by the EDAC circuitry all over checkouts duration.
- **Reference voltages:** This telemetry provides highly accurate information on the current performance of the CDMU's acquisition chain in view to possibly adjust the analog parameters calibration curves, and especially the entry accelerometers ones, on board. There are three stabilized reference voltages :
 - 4.54V and
 - 300mV and
 - 500mV

the later ones being set to be close to the voltage corresponding to the S_0 g-threshold, i.e. 522mV.

The Figure 5.5-6 hereafter shows the evolution over all checkouts of the stabilized voltages as acquired by the CDMU's. The telemetry of the CDMU's 5V-supply voltage is also displayed. This clearly demonstrates the very good operation of the analog acquisition chain. Also, no degradation from launch time is evidenced. These reference voltages are identical to the ones obtained for all previous checkouts.

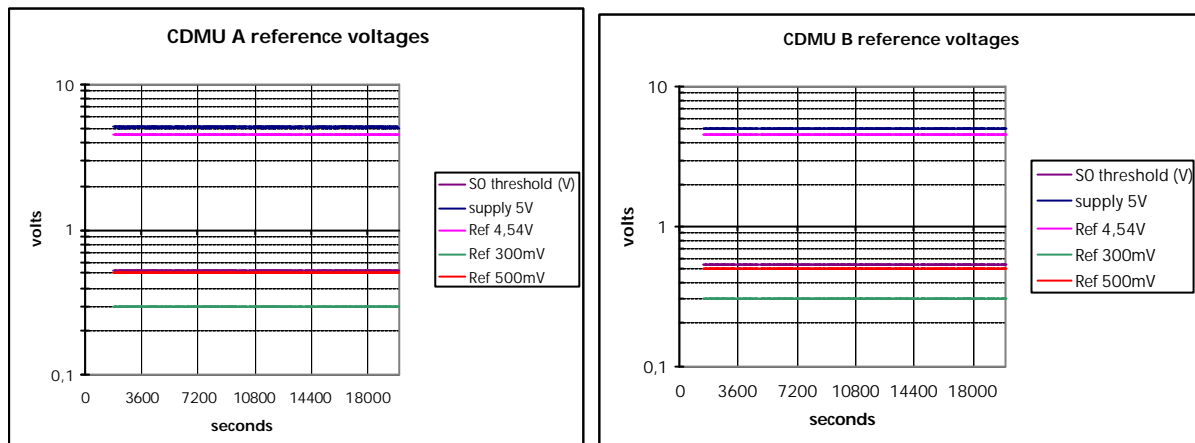


Figure 5.5-6: CDMU A & B voltages (5V is not stabilized)

5.6 ON BOARD SOFTWARE

5.6.1. SASW

This paragraph addresses the telemetry related to the SASW operation.

- **High Stack WaterMark:** This parameter aims at providing data on the stack usage by the SASW. It reports the 16bits address of the top of the stack, which shall be lower than the stack base address, i.e. 16#EFFF. Value reported during each checkout is in line with the requirement and basically in line with other checkout results.
- **SASW CUT Processing Time:** It reflects the processor load for each CUT. As expected, and as per all checkouts, processing time ranges from 16ms to 27ms, representing a nominal PSA data handling processor load of about 20 %.
- **DT Start/End Time, DT Start EXEC:** The DTStart parameter provides the time within the CUT when the Dead Time Start signal is received by the SASW. It shall be < 120ms. DTEnd parameter provides the time within the CUT when the DTStart interrupt processing stops. The interrupt processing duration is given by the **DTStart EXEC** parameter.

During all checkouts, on both chains, **DTStart** nominally happens generally 18.7ms after the CUT start; processing duration is in average 1.4ms, in line with the reference test results.

Few (2-3) unexplained excessive peaks in the DT interrupt processing time were noted during F7. No further effect has been noticed; this "anomaly" is considered minor.

- **FDI Start/End, FDI EXEC:** The **FDIStart** signal provides the time when a probe frame is received. **FDIEnd** provides the time when the FDI is serviced, while **FDI EXEC** simply indicates the duration of the interrupt servicing.

It shall be noticed that the **FDIStart** signal monotonously increases because of the probe (CDMU's) TM clock drift w.r.t. Cassini RTI.

Figure 5.6-1 shows this clock drift computed as a function of the temperature measured at CDMU A and B DC/DC converters level, over F3 to F12. The displayed drifts are absolute values, corrected with Cassini RTI shifts applicable for each checkout. These demonstrate that the TM clock on board the CDMU's is well within its stability requirement, and has not degraded over the time.

Processing duration, given by **FDI EXEC** parameter is in average 0.8ms, from all test results.

- **DMA Start/End, DMA EXEC:** The **DMAStart** signal provides the time when a Direct Memory Access interrupt is received. **DMAEnd** provides the time when the DMA interrupt is serviced, while **DMA EXEC** indicates the duration of the interrupt servicing.

The evolution of the telemetry related to DMA interrupt is quite similar to FDI related telemetry, with the same comments.

Duration of the interrupt servicing is, in average, 1.4ms, for all test results.

As a conclusion, we have [**DTStart EXEC + FDI EXEC + DMA EXEC = 3.6ms**], and the constraint for a correct software operation being [**DTStart EXEC + FDI EXEC + DMA EXEC < 4.5ms**] was fulfilled for all checkouts.

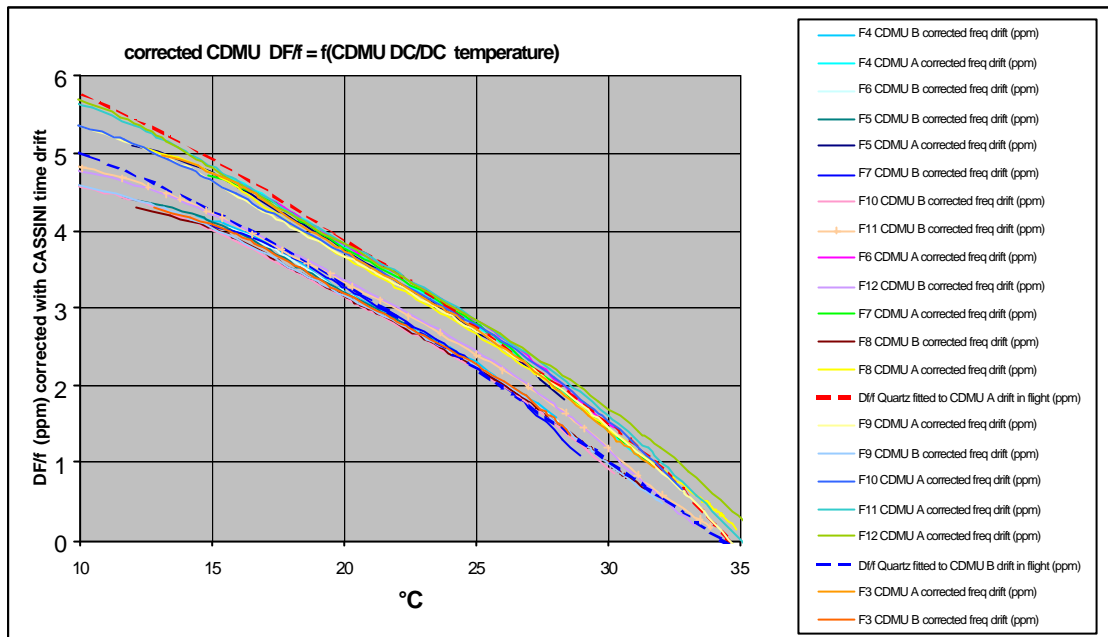


Figure 5.6-1: Computed CDMU A & B data clock drift wrt Cassini RTI

5.6.2 POSW

This paragraph addresses the telemetry specifically related to the POSW operation.

- **High Stack Water Mark:** This parameter aims at providing data on the stack usage by the POSW. It reports the 16 bits address of the top of the stack, which shall be lower than the stack base address, i.e. 16#EFFF. Value reported during each checkout is well in line with all other test results.
- **POSW CUT Processing Time:** It reflects the processor load for each CUT. The reported value is a worst case value over the 128 CUT major acquisition cycle and is actually the residual value of the CDMU's μ processor timer B at the end of the processing time.

As expected, processing time ranged from 56 ms to 60 ms, representing a nominal CDMU data handling processor load of about 55 % max. A slow increase of the processor load from T_0 time can be noticed; it reflected the fact that the TAT processing time is correlated to the current Mission Time.

Few spurious peaks in the processor load were noted during F7; this seemed to be an "artifact" of the TM reporting.

In total, the POSW processing showed a correct operation of the software over the whole checkout.

5.7 TEMPERATURE EVOLUTION

This section discusses telemetry measurements related to the thermal subsystem: probe and PSE temperatures in probe housekeeping, including unit's internal temperatures, plus probe and PSE temperatures in Cassini housekeeping.

5.7.1 Cassini temperature sensors

Figure 5.7-1 summarizes the evolution of the Probe, LNA's and SEPS (SIF side) temperatures at the end of the checkouts as measured from Cassini sensors.

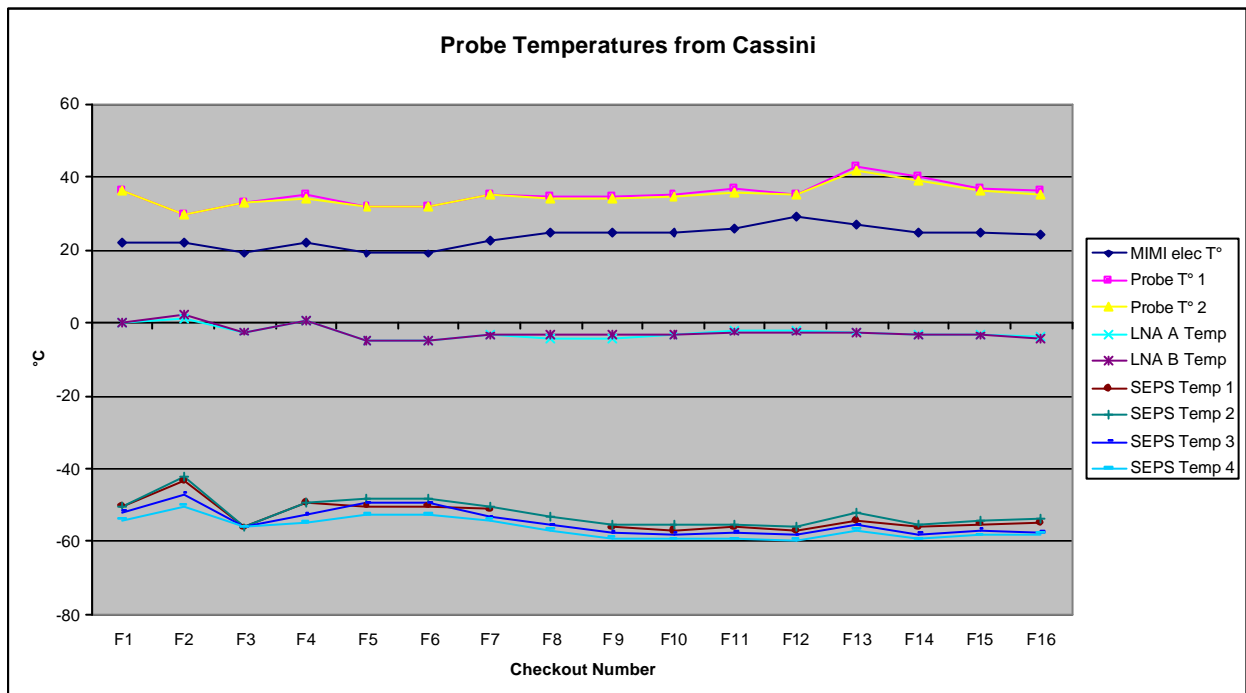


Figure 5.7-1: Probe and PSE final temperature evolution over checkouts

Those temperatures are in line with the predictions, and very stable over the different checkouts, and the small variations can be attributed to changes in the Sun-Spacecraft distance (see Fig 4.1-1) and Cassini attitude changes.

The Figure 5.7-2 shows the evolution of the PSA A and B initial temperatures over the checkouts.

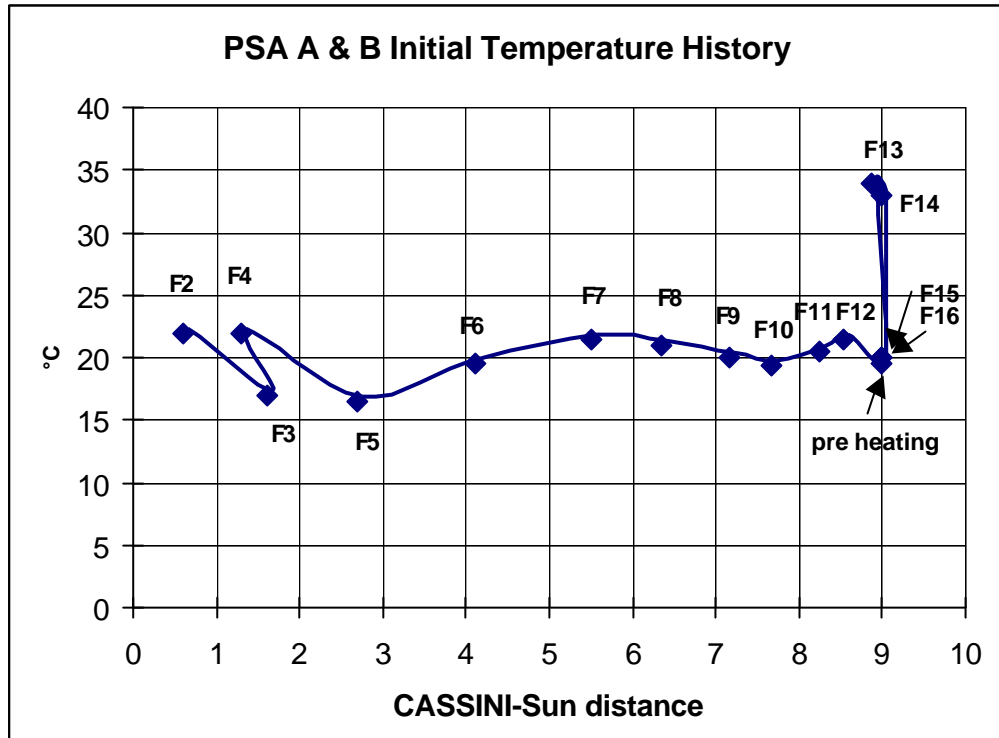


Figure 5.7-2: Initial PSA A & B temperature evolution over checkouts

Note that Fig 5.7-2 indicates the temperature at the start of the checkout sequence; as far as F13 and F14 are concerned, the checkout sequences were preceded by 2 to 3 hours long MTU drift tests, which explains the higher initial temperature.

The PSA A and B temperature increase during the various checkouts was of about 20°C independently from the duration of the checkouts. At the end of the checkouts, PSA A and B temperature range was 40 to 42°C.

5.7.2 Probe temperatures

The temperature values, in °C, acquired by the Huygens Probe System thermistors are summarized in the Figures hereafter.

a. Descent module external units

The Figure 5.7-3 summarizes the evolution of the SEPS (PIF side), PJM and PDD temperatures at the end of the checkouts.

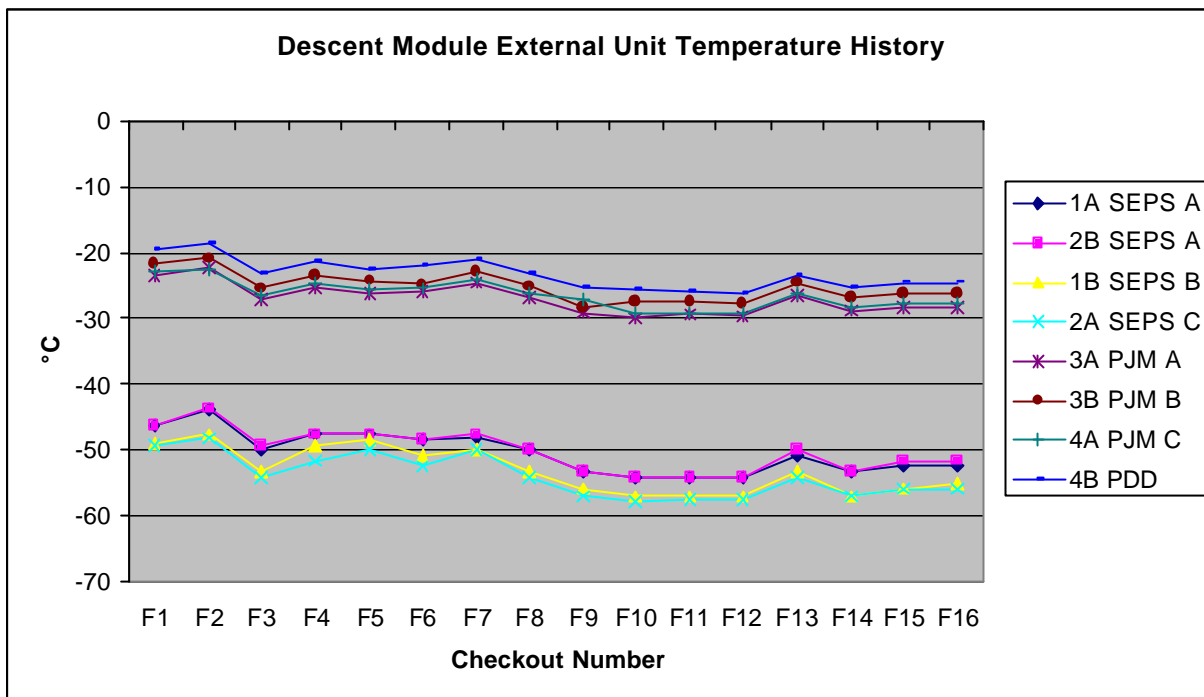


Figure 5.7-3: Final temperature evolution of descent module external sensors over checkouts

Figure 5.7-4 displays the evolution of the SEPS (PIF side) initial temperatures as a function of the Sun-S/C distance for the different checkouts. The amplitude of variation is limited to ~10°C over the 7 years cruise phase. The “peaks” appearing at F13 for all measured temperatures are clearly linked to the long F13 duration (see Fig 4.1-2).

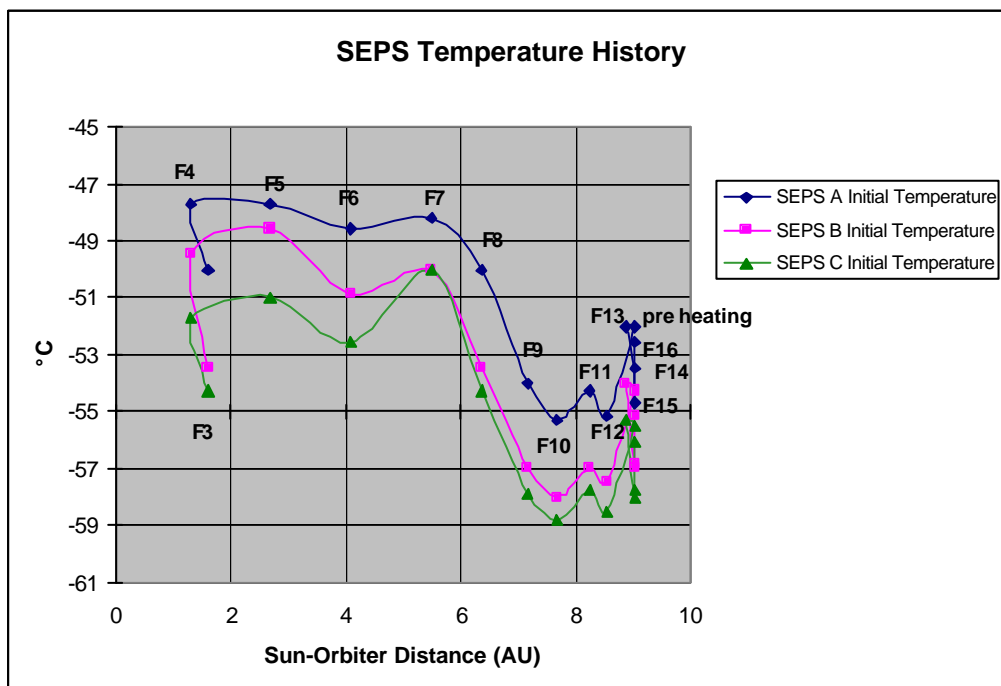


Figure 5.7-4: Initial SEPS temperature evolution over checkouts

b. Descent module internal units

The Figure 5.7-5 summarizes the evolution of the temperatures of PCDU, batteries, transmitters, GCMS, TUSO, DISR and foam (external and internal) at the end of checkouts.

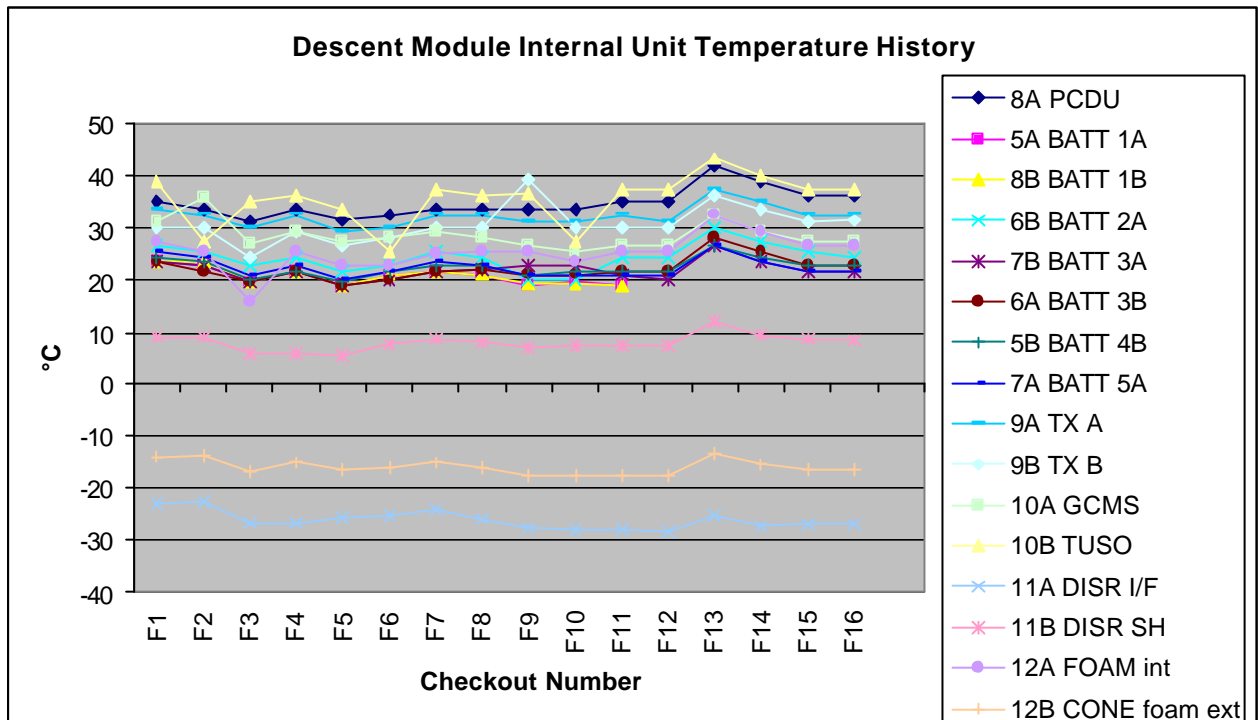


Figure 5.7-5: Final temperature evolution of descent module internal units over checkouts

The TUSO temperature is affected by the type of checkout (CO1a, CO1b or CO2), since TUSO is OFF during CO1 and CO1a. As far as the other units are concerned (GCMS, TX's, BATT, PCDU), the final checkout temperatures are stable, mainly modulated by the duration of the checkouts (see Fig 4.1-2). No temperature has never exceeded the units acceptance limit.

The difference between FOAM int and CONE temperatures is representative of the thermal efficiency of the foam.

c. Probe internal units temperatures

The Figure 5.7-6 summarizes the evolution of the temperatures measured inside the units, RUSO and TUSO, PSA, Tx HPA's and CDMU DC/DC Converters, at the end of checkouts. They are consistent with temperature measured externally (see point b), with the following remarks :

- The evolution of TUSO and RUSO internal temperature reflect the power status of the units, depending on the checkout type,

- The Tx HPA temperature remain low because the HPA's are OFF in cruise phase.

Note that the CDMU A & B DC/DC temperatures have been used to characterize the drift of the CDMU's TM oscillator (see Fig 5.6-1).

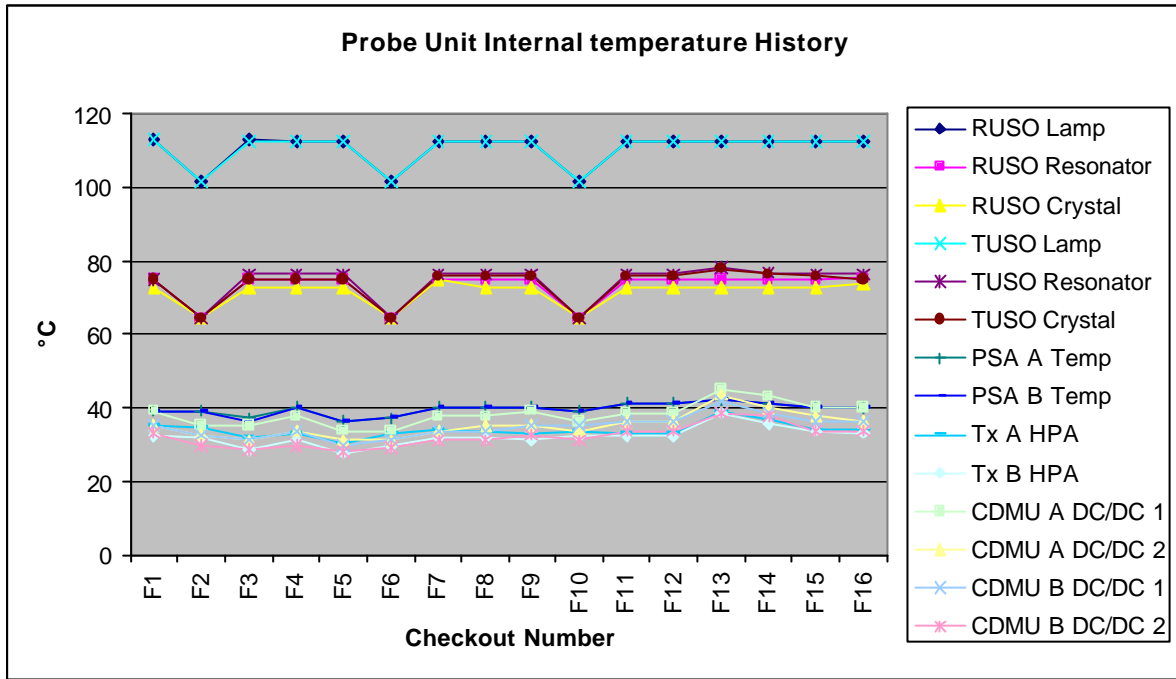


Figure 5.7-6: Final internal temperature evolution of probe units over checkouts

Conclusion:

The initial steady state temperatures are mostly related to the Sun - spacecraft distance and to the Huygens Sun illumination.

F13 and F14 are specific cases : the temperature of the internal units compared to F12 ones was increased by ~5°C and ~2°C respectively for units switched off, and by ~7 to 10°C and 2.5 to 7.5°C respectively for units switched on. This is consistent with the fact that a 2 to 3 hours long MTU drift test was run before these checkouts leading to a significantly warmer start temperature.

The Figure 5.7-7 illustrates this overall behavior by showing the evolution of the PCDU initial temperature as a function of the Sun-Spacecraft distance, for the different checkouts.

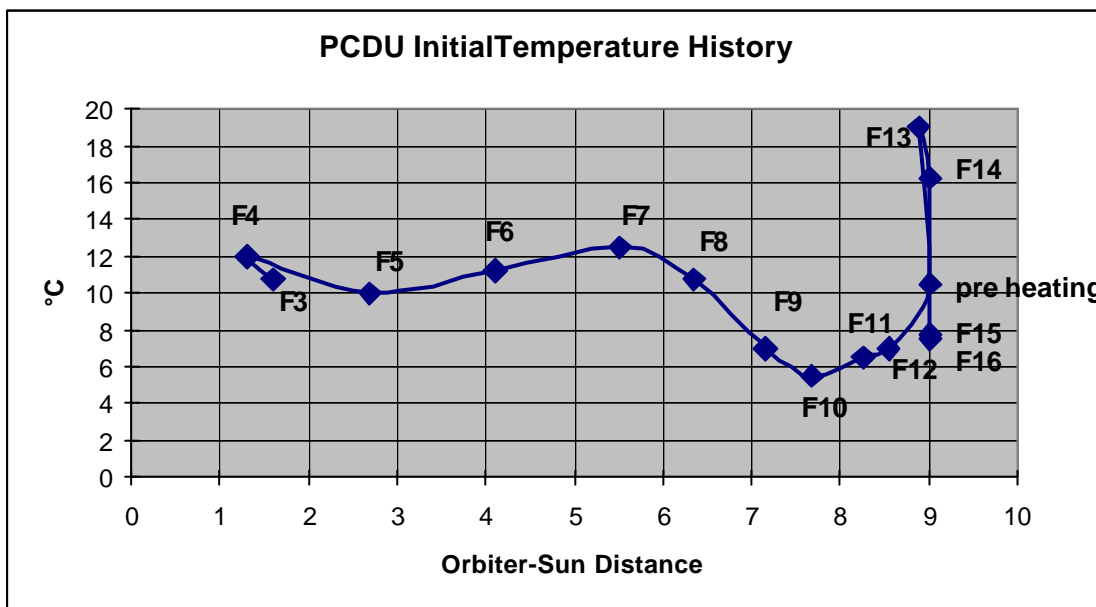


Figure 5.7-7: Initial PCDU temperature evolution

The F6 and F7 temperature increase can be explained by considering that Huygens was completely shadowed by the Cassini HGA during F1 to F4, while it was partially subjected to - limited - solar illumination during F6 and F7.

F8 as F9, F10 and F11, reflect the effect of the Sun illumination decrease with the distance. Between F10 and F11, in relative, the Cassini-Sun distance has only slightly increased, and the initial temperature change is therefore minimum. This trend is valid also for F15 while F13 and F14 reflect the longer sequence duration due to MTU drift test; despite the overall test duration all temperature have stayed within the acceptance limits.

The temperatures trends are in accordance with RD02, computed after the thermal model adjustment in July 98 (RD01).

They are in addition very consistent considering the respective checkouts duration's (see Figure 4.1-2). This is clearly illustrated in Figure 5.7-8 for the PCDU case.

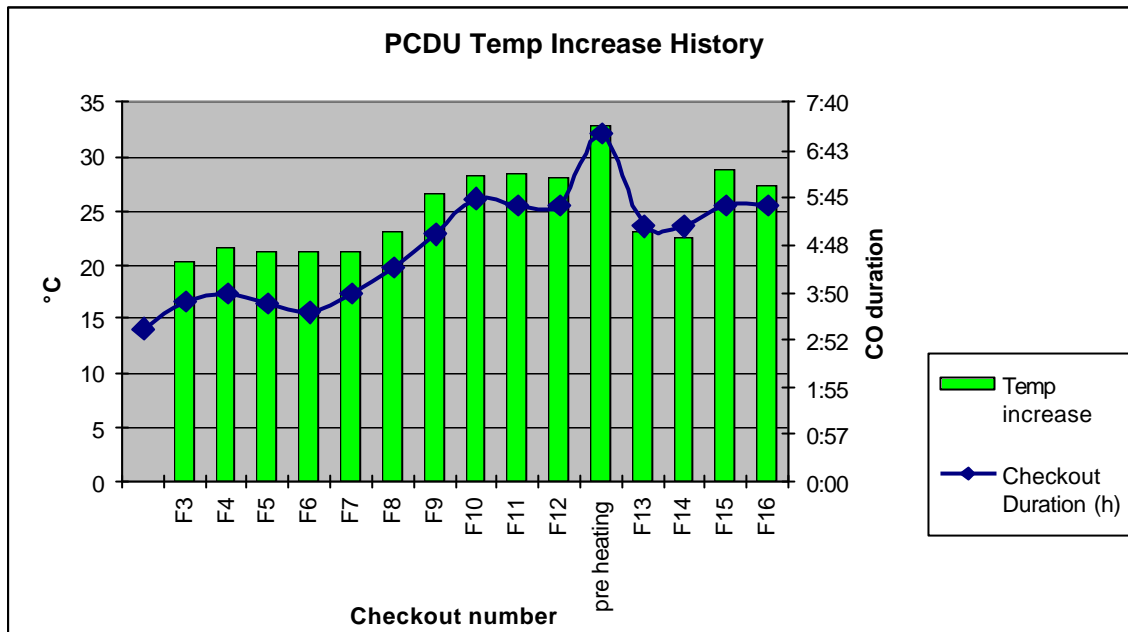


Figure 5.7-8: Initial PCDU temperature evolution wrt checkout duration

The overall probe system thermal behavior is therefore considered nominal over all the checkouts.

5.8 EXPERIMENTS STATUS WORD

The evolution of the Status Word for each instrument is similar to its evolution from one checkout when compared to the reference ones (CO1 and CO2).

Experiments detailed behavior analysis shall be found in the PI's test reports : no anomaly which could impact the Probe System operation have never been notified.

6. CASSINI CHECKOUTS

This chapter deals with the review of the technical issues raised, related to Cassini and especially Cassini instruments operation, which have had an impact on the Huygens Probe System.

A concern was first raised (addressed in F3 and F4 reports) about the Radio Front End (RFE) unit thermal behavior during operation of the Cassini Radio Science experiment (RFE temperature increases, even when Huygens PSA's in OFF, when the Radio Science experiment is operated). It was closed based on an analysis performed by ESTEC, showing that the parts and processes used in the RFE were likely to comply with any heating induced by RSS operations.

Also, belonging to that category, a statement was requested on the possibility to maintain nominally six of the Cassini instruments in "on" but "sleep" mode condition during future probe checkouts. EMC and 1553 orbiter data bus issues have mainly been addressed via the analysis of documentation provided by JPL and dealing with:

- 1553 bus muting
- EMC measurements recorded during " quiet test " on ground.

As mentioned in the F7 report, it was stated that:

- the mute mode proposed to be used to prevent data generation from Cassini instruments during probe checkouts was fully satisfying Huygens request.
- the EMC results from ground testing were not considered to properly cover the conditions planned to be exercised in flight.

A dedicated flight test has been designed to assess the Cassini instruments sleep mode impact on a " dummy " probe checkout.

This test has been run in August 2001, and has demonstrated that the probe was behaving nominally, and thus a flight checkout could be performed safely when Cassini instruments were in sleep mode. As a consequence, checkouts from F8 were run with Cassini instruments in sleep mode.

7. CONCLUSION

The synthesis of the 16 checkouts run as part of the Huygens Cruise phase has shown a nominal and stable operation of all Huygens subsystems.

The formally unexplained noise level on CASU accelerometers has been demonstrated as fully acceptable from a system point of view.

The RF link between Probe and PSA has been nominal, after explanation of the F1 & F2 anomaly, with an AGC signal in accordance with the expected value.

The 3 timers of the MTU have been programmed and successfully exercised. The timers accuracy has been characterized and proved to be well within their allocated budget.

The 1st batteries depassivation sequence run after F15 has shown that the status of all 5 batteries is excellent and that no capacity degradation is expected. **This has been confirmed by the 2^d depassivation sequence run after F16, and permits to recommend the baseline implementation of the Probe pre heating option.**

To conclude, the Huygens Probe System status at the end of the cruise phase, after F16, is nominal,

- all redundancies are in place (the Probe System IS SPF tolerant for the mission)
- **the 5 batteries health status is nominal**
- the Probe has demonstrated very stable performances for all its functions over 3h to 5h35min of operation

and fully consistent with the Huygens Nominal mission including the pre heating option.